applied sciences

MDPI

Perspective

Fluorinated Polymers for Photonics—From Optical Waveguides to Polymer-Clad Glass Optical Fibers

Leonid M. Goldenberg [1,2,*], Mathias Köhler [2] and Christian Dreyer [1,2,*]

[1] Department Fiber Composite Material Technologies, Faculty of Engineering and Natural Sciences, Technical University of Applied Sciences Wildau, Hochschulring 1, 15745 Wildau, Germany
[2] Fraunhofer-Institute for Applied Polymer Research, Research Division Polymeric Materials and Composites PYCO, Schmiedestr. 5, 15745 Wildau, Germany; mathias.koehler@iap.fraunhofer.de
* Correspondence: leonid.goldenberg@th-wildau.de (L.M.G.) christian.dreyer@th-wildau.de (C.D.)

Featured Application: Optical waveguides for polymer-based optical microchips and polymer cladding for fused silica fibers.

Abstract: In this paper, our work in the field of fluorinated UV-curable polymers is reviewed. These polymers possessing tunable low refractive indices and low optical propagation losses for telecommunication wavelengths are intended to be used as core and cladding materials for the fabrication of passive channel waveguides in optical microchips on the polymer platform. This application requires low thermo-optic coefficients. With this goal, we used a combination of fluorinated polymers with low-refractive index inorganic nanoparticles of SiO_2 and MgF_2. Another application requiring extremely low refractive indices is polymer cladding for optical glass fibers. UV-curable fluorinated monomers/oligomers were used.

Keywords: fluorinated acrylate; nanoparticles; nanocomposite; thermo-optic coefficient; optical propagation losses; glass fiber; polymer cladding

Academic Editors: Malgorzta Gil-Kowalczyk and Paweł Mergo

Received: 20 December 2024
Revised: 4 February 2025
Accepted: 5 February 2025
Published: 10 February 2025

Citation: Goldenberg, L.M.; Köhler, M.; Dreyer, C. Fluorinated Polymers for Photonics—From Optical Waveguides to Polymer-Clad Glass Optical Fibers. *Appl. Sci.* **2025**, *15*, 1790. https://doi.org/10.3390/app15041790

1. Introduction

Organic polymers containing C-F bonds found a wide application in photonics. Low refractive indices and apparently low propagation optical losses at the communication wavelength of 1550 nm are the most interesting properties of fluorinated polymers in view of applications in optics. Low absorption in the wavelength region ca. 1550 nm is the main challenge for the material, as this absorption contributes mainly to the optical propagation losses. The presence of –OH and –NH groups has to be avoided to reduce the propagation losses in this wavelength region (these chemical bonds absorb very strongly in the near infrared region). Therefore, polyurethanes, epoxy resins thermally cured by amine-containing hardeners, phenolic resins and polyamides are generally not considered for such applications. C–H bonds are normally present in almost all organic polymers, and they also absorb in this region. However, the absorption caused by C–H is a result of the overtones of the C–H stretching vibration and is consequently two orders of magnitude lower than the first overtone of –OH or –NH vibration lying exactly in the 1550 nm region. Nevertheless, the absorption of –CH groups in the infrared region also influences optical propagation losses in optical devices. The use of fluorinated and highly fluorinated polymers leads to a reduction in optical propagation losses, making

fluorinated polymers versatile for integrated optical devices. In addition, the substitution of hydrogen for fluorine or another halogen also reduces the concentration of C-H bonds.

Therefore, here we review our previous research in two application areas involving fluorinated UV-cured thermosetting polymers, namely, their application as core and cladding layers for the fabrication of channel waveguides used in optical microchips [1–5] and their application as cladding layers for optical glass fibers [4–6].

While for the first application, tunability of the refractive index and low propagation losses are important features, for the second application, a low refractive index is the most important. Two classes of polymers (oxirane-containing fluorinated polymers and a monomeric mixture of fluorinated acrylates) are used for passive optical waveguides, with the emphasis in our own work being on nanocomposites [1–3].

2. Fluorinated Polymers for Passive Optical Waveguides

Currently, several polymer materials have been developed for photonic applications. Such optical polymers have become state-of-the-art, particularly in the form of polymer optical fibers [7]. Linear polyacrylates such as poly(methyl methacrylate) (PMMA) have primarily been used, but they exhibit significant aging effects at moderate temperatures above 75 °C. A fluorinated polymer is used as optical cladding to enable waveguiding. Modified PMMA from Toray Industries [8] shows higher long-term thermal stability and heat resistance. Polymer optical fibers based on linear PMMA show low propagation losses of 0.0016–0.003 dB·cm^{-1}, but only in the wavelength range between 650 and 670 nm [9]. This limits their usability to lengths of less than 100 m, in contrast to optical glass fibers, which can transmit data over many kilometers (in the wavelength range around 1550 nm). In addition, PMMA can absorb up to 1.5% of water, which has a negative effect on its propagation losses [7]. The use of these materials, especially PMMA, for integrated optical components has already been described in the literature [10–12] and reviewed in 2002 [13]. However, these materials have several disadvantages, especially high losses in the wavelength range around 1550 nm, which are mainly due to the harmonics of the C-H bond [7]. For the wavelength range around 1550 nm considered here for polymer-based optical microchips, the loss values are typically worse than those of PMMA. In addition, none of these materials are cross-linked, which makes processing into integrated components difficult or even impossible (e.g., re-dissolution of the lower cladding layer by the solvent of the waveguide layer). In addition, the refractive index is too high and there is no second material available to provide a sufficient index contrast. Thermoplastic polymers also have a very high thermo-optic coefficient (TOC) [14].

In addition to the materials mentioned above, several other systems for integrated optical components have been described in the literature. Benzocyclobutene from Dow Chemicals has too high optical losses for applications around 1550 nm [15]. Perfluorocyclobutane polymers, originally developed by Dow as low-k materials for microelectronics, have been further developed by the US research group led by D. W. Smith and used for various optical and other applications [16–18]. They exhibit low optical losses at 1550 nm (sometimes as low as 0.2 dB·cm^{-1} at 1550 nm), but their adhesion to silicon is poor.

Fluorinated acrylates from Allied Signal [19] have low propagation optical losses at 1550 nm, but there are no material pairs with a sufficiently high index contrast.

Several classes of polymers were used in our previous research [20,21]. Functional prototypes of integrated optical components based on monomodal polymer optical waveguides were developed using different polymer classes for telecommunication applications, particularly in the wavelength range around 1550 nm.

Depending on the respective integrated optical components, different polymers were developed. These included fluorinated (meth)acrylate co-polymers, polycyanurates, new triazine-containing polymers (e.g., triazine acrylates), perfluorocyclobutane (PFCB)

polymers and PFCB–polycyanurate hybrid polymers. The layers were prepared by spin-coating of prepolymer solutions, whereby the refractive index contrast Δn = 0.008–0.020 between the cladding and the core was achieved using specially designed co-polymers. The polymer systems developed possessed very reproducible process characteristics. With polycyanurate co-polymers, optical propagation losses below 0.3 dB·cm^{-1} at 1550 nm could be achieved, although the processability was not sufficient.

The partially fluorinated (meth)acrylate co-polymers, which can be processed on silicon and show good film formation properties, proved to be particularly promising, especially due to their good processing properties. The optical losses at 1550 nm were still too high (0.8 dB·cm^{-1}), and acrylates have a rather limited temperature resistance.

Silicones, some of which are deuterated, have also been used as waveguide materials in the past [22,23]. The disadvantages were non-optimal optical losses, a tendency to swell in media and a thermo-optic coefficient about 2.5 times higher than that for PMMA [10].

Ormocer® hybrid materials have high thermal stability and show moderate optical losses of approx. 0.6 dB·cm^{-1} at 1550 nm. Their refractive index is above 1.51 at 1550 nm, even in the case of fluorinated systems [24].

The South Korean company ChemOptics [25] offers a material system that shows low optical losses (0.35 dB·cm^{-1} at 1550 nm) in the layer waveguide and good adhesion to silicon. However, the TOC is not low (−(1.5–2.2) × 10^{-4} K^{-1}).

Photochemically active polymers are a broad branch of polymer science and are used as UV-curable thermosets in passive and active optical waveguides, optical cladding for glass fiber, photoresists and composites. From a chemical point of view, two main reactions are the radical photochemical polymerization of carbon double bonds (often acrylates) and the ring-opening polymerization of oxiranes using photoacid generators.

Photopolymerization of the double bond is used in the above-mentioned commercial materials from ChemOptics for passive optical waveguide fabrication [25], while photochemical cross-linking of oxirane-containing polymers is the typical reaction in negative photoresists.

In general, a planar optical waveguide consists of two materials. The core material (n = 1.48–1.50) is clad with another polymer material (called cladding, n = 1.45) [26,27]. The refractive index of cladding is usually close to that of fused silica (1.444 at 1550 nm). The refractive index contrast between the core and the cladding materials (0.05, 0.03 or lower) is determined by the application. The general design of a channel optical waveguide is shown in Scheme 1.

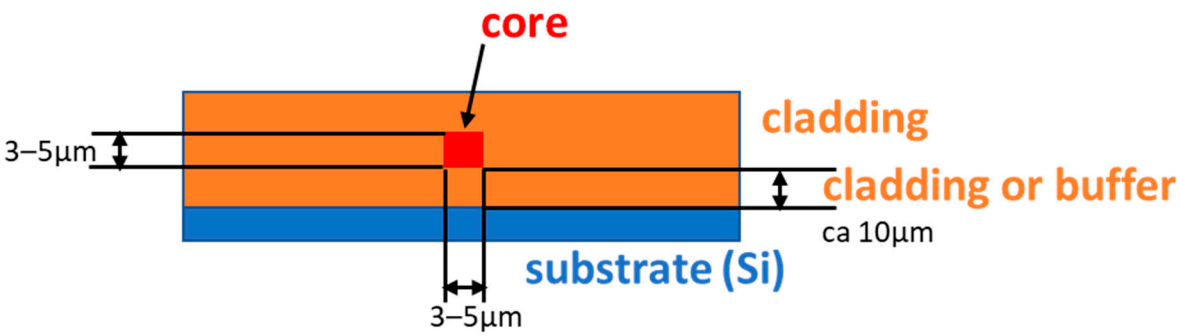

Scheme 1. Schematic cross-section of channel optical waveguide.

Passive optical waveguides are used in the optical microchip on the polymer platform (Scheme 2). They are shown in dark blue in Scheme 2. A passive optical waveguide serves as a connection between elements of a microchip similarly to wire in an electronic

chip. Other elements could be filters, switches, gratings, distributors, etc. An optical fiber is connected to a passive waveguide via a U-nut.

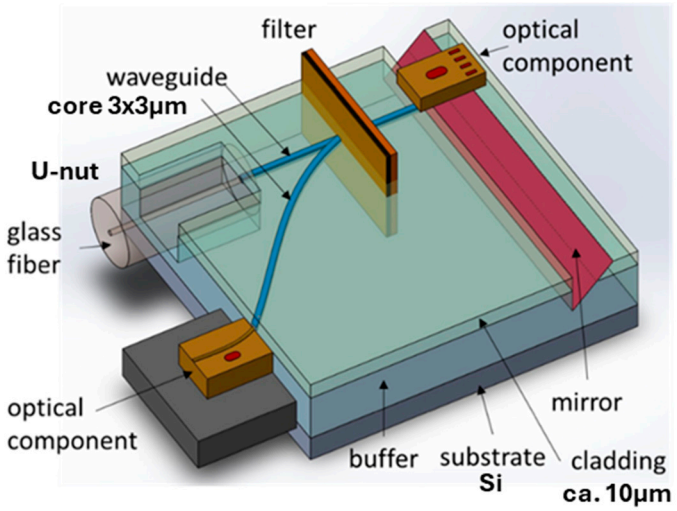

Scheme 2. Scheme of an optical microchip on a polymer platform, where dark-blue lines represent passive polymer optical waveguides.

Different fabrication procedures can be used for such waveguide fabrication, including direct photolithography, where the core layer serves as a photoresist (Scheme 3).

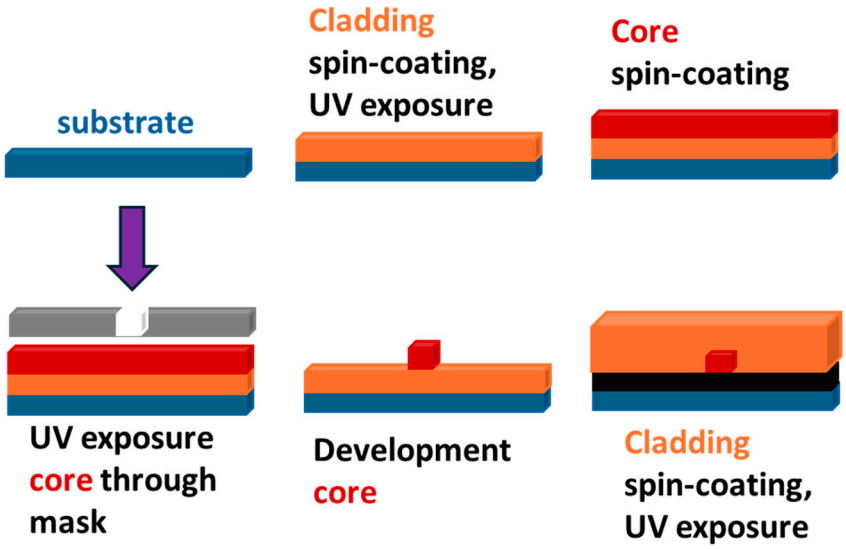

Scheme 3. Direct photolithographic fabrication of planar optical waveguide.

In the case of viscous monomeric mixtures, such as the material from ChemOptics [25], usually more complicated procedures involving reactive ion etching are applied (Scheme 4).

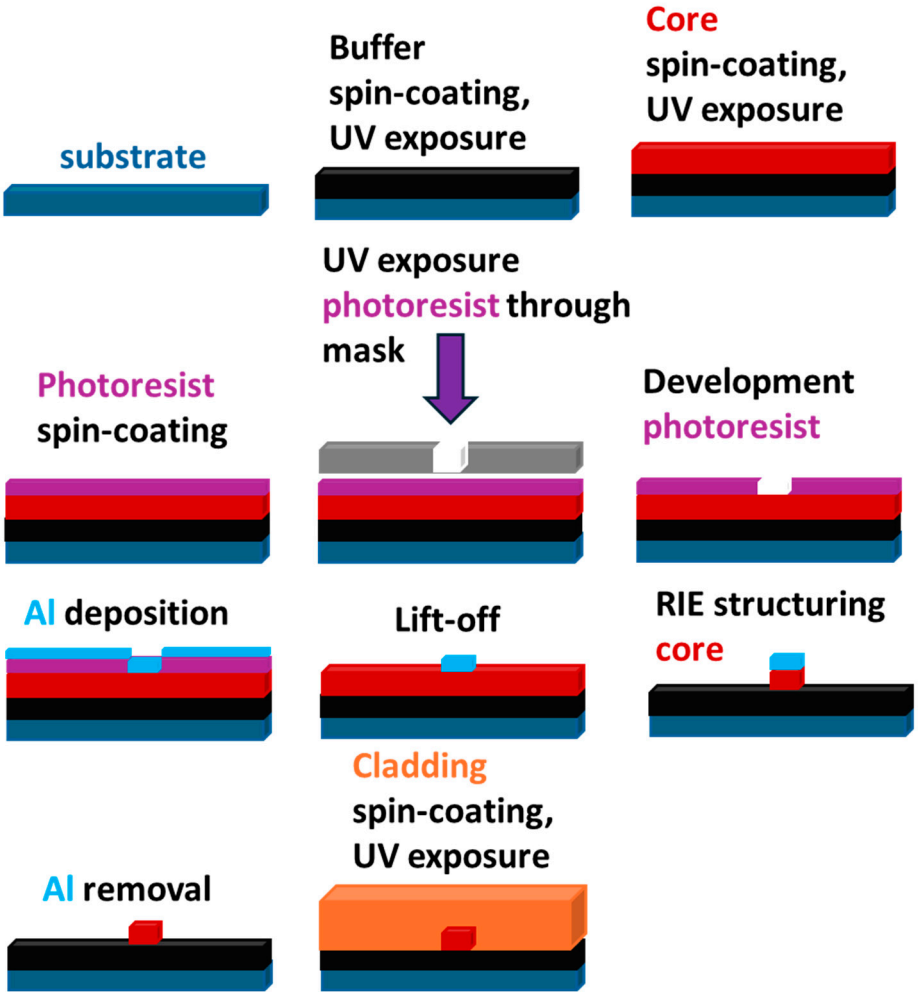

Scheme 4. Schematic representation of the process of optical waveguide fabrication using reactive ion etching (RIE).

It is also possible to apply soft lithography techniques (microcontact printing or micromolding in capillaries [13]).

2.1. Material Based on a Halogenated Acrylate Mixture

A representative composition of the formulations is shown in Scheme 5. The chemistry is based on photochemical cross-linking via radical polymerization of double bonds (mostly in acrylate groups or styrene-type derivatives).

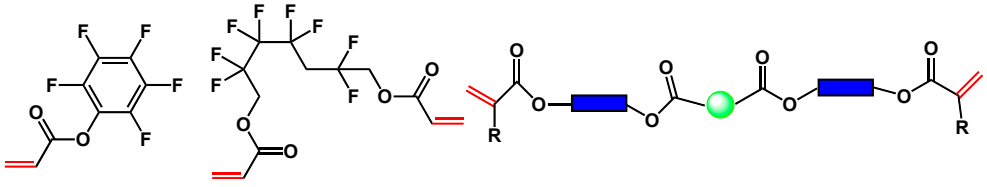

Scheme 5. Typical examples of fluorinated monomers of acrylate type and viscous polyester acrylate for the formulation of liquid mixtures for optical waveguide fabrication.

We were able to reduce optical propagation losses and refractive indices using highly fluorinated components. Other components (shown in the middle of Scheme 5), which were different viscous oligomeric biacrylates, were used to adjust the rheological properties. Finally, the refractive index and viscosity were adjusted to meet the refractive index and thickness requirements of the core and cladding layers. Different viscous acrylates,

such as Merimer from MIWON, Sartomer from Arkema, Ebecryl from Allnex and OGSOL from Osaka Gas Chemical, were used. These viscous oligomers were selected based on their FTIR spectra to avoid O-H or N-H bonds and according to their viscosity.

All optical parameters were measured using m-line spectroscopy with a Prism Coupler System Metricon 2010/M (Metricon Corporation, Pennington, New Jersey, USA). The optical propagation losses of the planar waveguides on fused silica slides were obtained by measuring the scattered and transmitted light intensity as a function of the propagation distance along the slide [28]. This is shown in the image in Figure 1 for visible He-Ne laser light (633 nm). A schematic of the method is also shown in Figure 1. An example of optical loss measurement for core materials is shown below, in Figure 1. Measurement of optical losses at 1547 nm for materials based on acrylate mixtures exhibited values of 0.3–0.6 dB·cm^{-1} (core) and 0.4–0.5 dB·cm^{-1} (cladding).

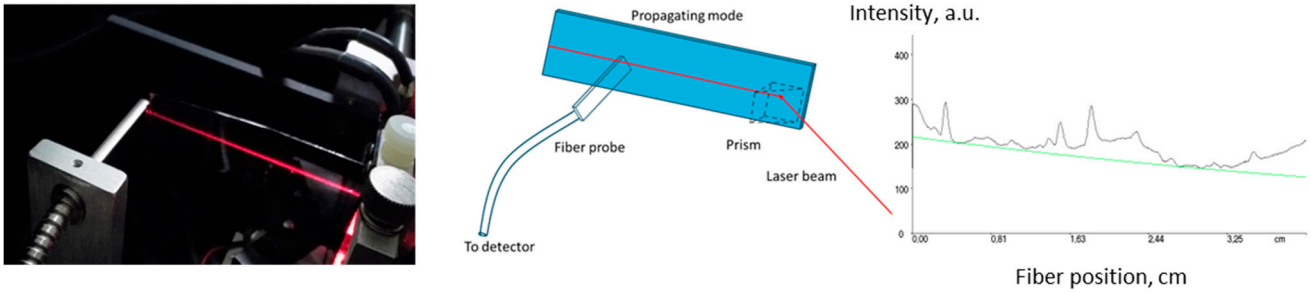

Figure 1. Measurement of optical propagation losses by transmitted and scattered light intensity: image of measurement at 633 nm, schematic of measurement and measurement at 1547 nm for core material with n = 1.5 of acrylate monomer mixture based on Ebecryl 150 oligomer (0.6 dB·cm^{-1}) (green line represents exponential fit).

The thermo-optical coefficient (TOC) was determined by measuring the refractive index at different temperatures using a temperature-controlled prism in the same Metricon system. It is the tangent of the linear plot of the dependence of the refractive index on the temperature. The kick in the curve usually shows a phase transition in the material (glass transition or melting). Examples are shown in Figure 2.

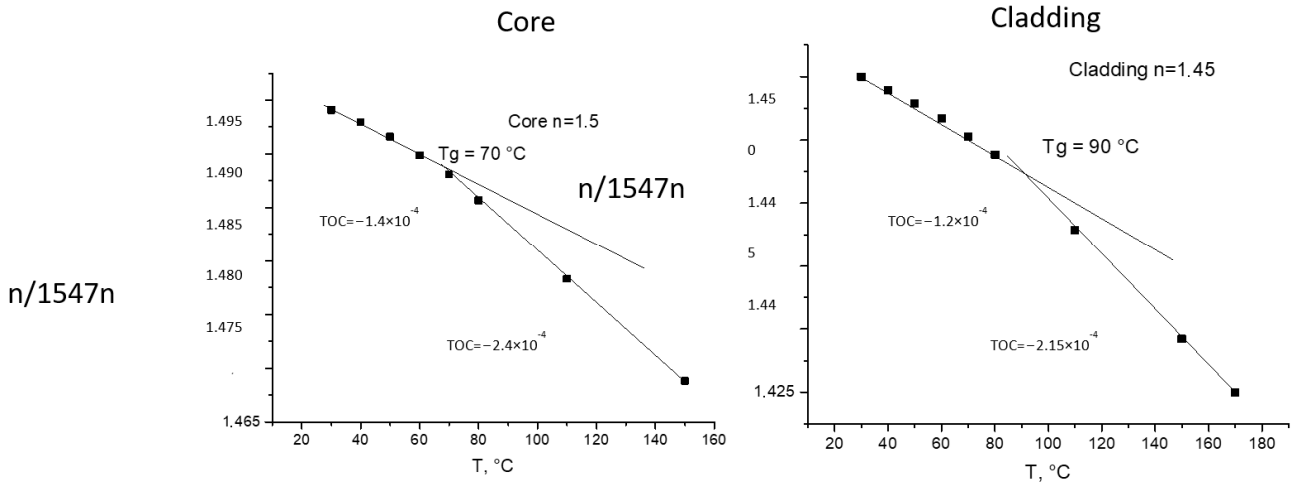

Figure 2. Measurements of TOCs of core and cladding materials with m-line spectroscopy at 1547 nm.

The formulation of the monomer mixtures was adjusted for the required refractive index. Most of the studied mixtures provided layers of sufficient optical quality and thickness for complete optical characterization (n, thickness, TOC, glass transition temperature, T_g and optical propagation losses). The fabrication of channel waveguides using RIE technology (Scheme 4) was also possible. Photochemically cured polymeric materials of this type exhibited TOC values of −(1.3–1.5) × 10^{-4} K^{-1}, which were lower than those of commercial materials from ChemOptics (−(1.5–2.2) × 10^{-4} K^{-1}) [25].

2.2. Glycidyl-Containing Polymer Materials

It has already been discussed above that the presence of C-F bonds leads to a decrease in optical losses and refractive indices. However, the presence of other C-halogen bonds (C-Cl or C-Br) also leads to a decrease in optical propagation losses and an increase in the refractive index. By using different halogenated derivatives, it is possible to tune the refractive indices of polymer layers, which is especially important for the core layer. Here, we used the co-polymer based on acrylate; fluorinated, chlorinated and brominated acrylates; or other compounds containing double bonds (for example, styrene-type compounds). Changing the concentrations of F, Cl and Br allowed a reduction in optical losses and tuning of the refractive indices for core (n = 1.48 or 1.5) and cladding polymers (n = 1.45). Adjustment to the required layer thickness (10 μm for cladding and 3 μm for cores) was also possible by changing the concentration of polymers in the solution. To cross-link polymers in layers and to make the polymer layers patternable either by direct photolithography or by reactive etching (Schemes 3 and 4), glycidyl methacrylate or acrylate was used as one of the co-monomers in radical co-polymerization. The oxirane group in the polymer chain is typically used in negative photoresists and allows direct structuring of such polymers via photolithography. To decrease optical losses, the content of glycidyl comonomers must be kept to a minimum, while the photochemical reaction of this group leads not only to cross-linking of the polymer chain, rendering the polymer insoluble, but also to the formation of O-H groups. These groups increase the optical propagation losses. Some examples of useful co-monomers are collated in Scheme 6.

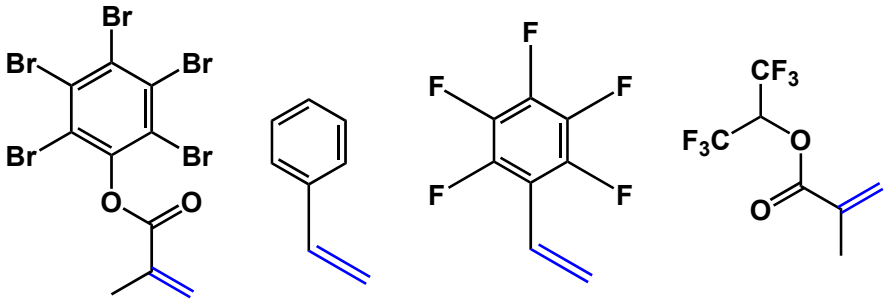

Scheme 6. Examples of double-bond-containing monomers with Cl(Br) increasing refractive index and F decreasing refractive index.

The scheme of polymer fabrication (radical co-polymerization) and application for the manufacture of waveguide layers (UV-curing in the layers) is shown in Scheme 7.

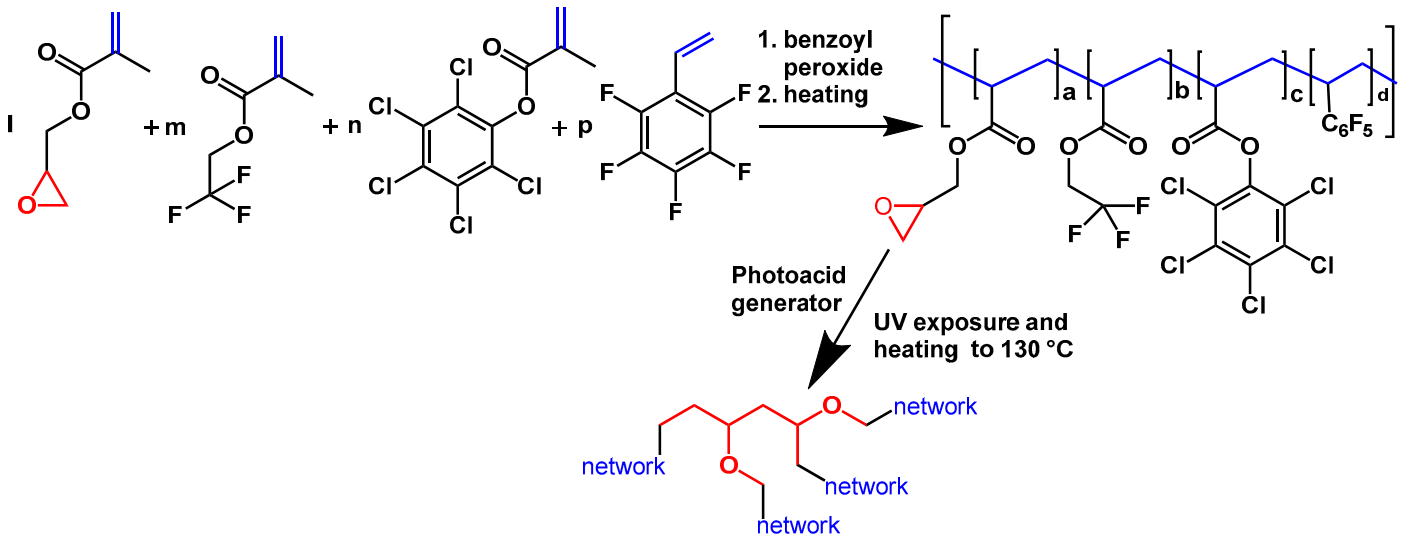

Scheme 7. Polymerization followed by UV curing (cross-linking) for the fabrication of waveguiding co-polymers and their photolithographic processing.

The TOC values (0.65–0.85 × 10^{-4} K^{-1} for cores and 0.8–1.0 × 10^{-4} K^{-1} for cladding) were measured (see example in Figure 3).

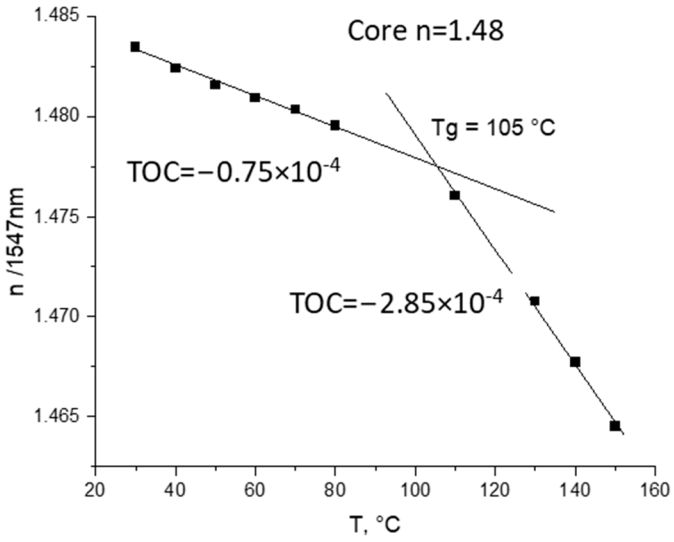

Figure 3. Measurements of TOC for core polymer obtained according to Scheme 7 with m-line spectroscopy at 1547 nm.

Optical propagation losses of 0.5–0.7 dB·cm^{-1} at 1547 nm (core) and 0.6–0.8 dB·cm^{-1} (cladding) were achieved. Some examples of loss measurements are shown in Figure 4.

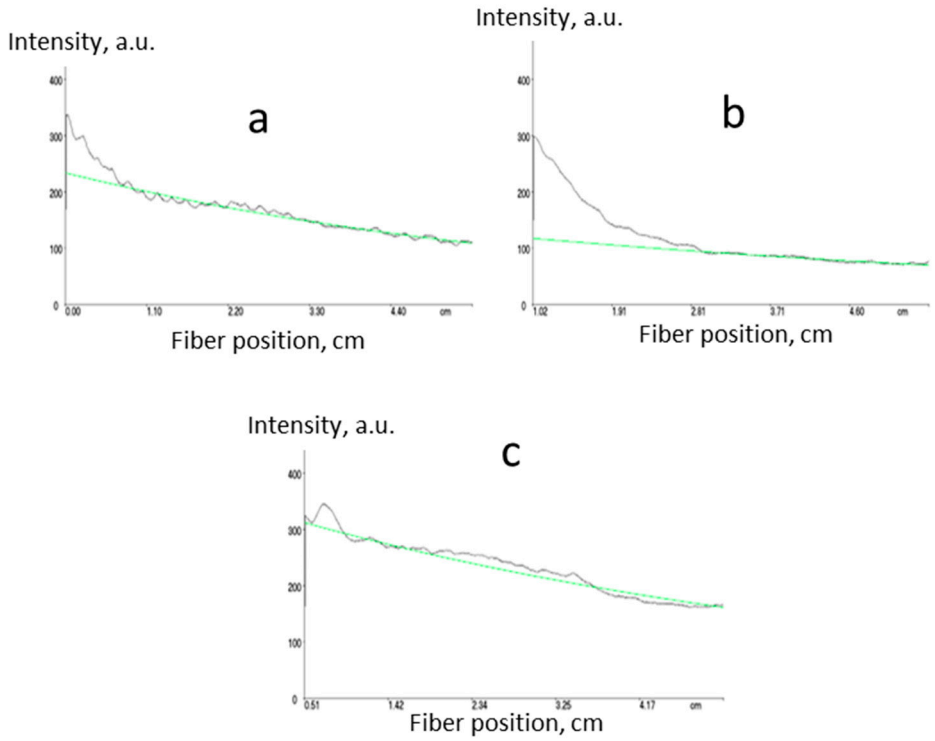

Figure 4. Measurement of propagation optical losses for core n = 1.5 ((**a**) 0.6 dB·cm^{-1}), core n = 1.48 ((**b**) 0.5 dB·cm^{-1}) and cladding n = 1.45 ((**c**) 0.6 dB·cm^{-1}) polymers prepared according to Scheme 7 using m-line spectroscopy at 1547 nm (green lines represent exponential fits).

By using different monomers, such as styrene or 4-chlorostyrene, and reducing the glycidyl acrylate content to 5 wt.%, it was possible to reduce the optical propagation losses (Figure 5).

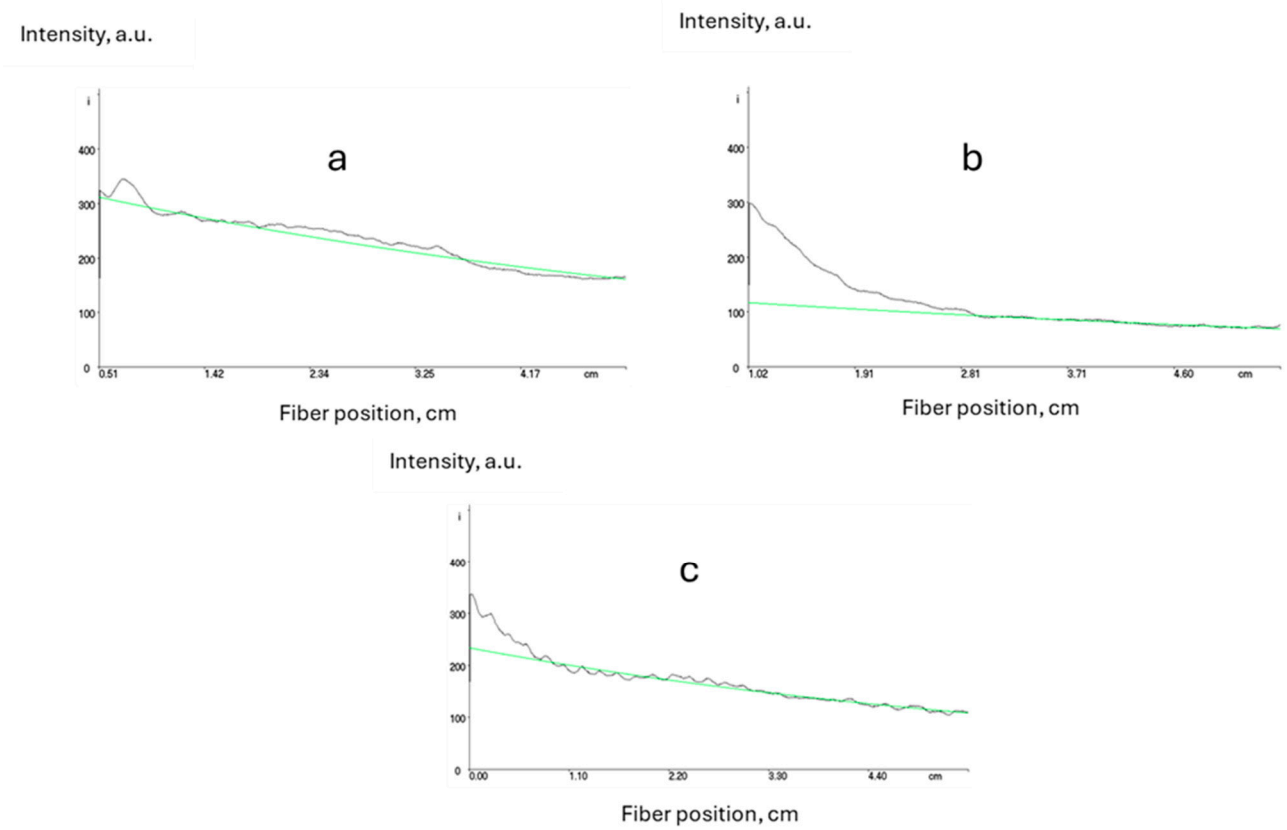

Figure 5. Measurement of propagation optical losses for core ((**a**) n = 1.5, 0.4 dB·cm^{-1}), core with styrene ((**b**) n = 1.48, 0.5 dB·cm^{-1}) and cladding with only 5%wt of glycidyl acrylate ((**c**) n = 1.45, 0.4 dB·cm^{-1}), (green lines represent exponential fits).

Examples of photolithographic processed core materials are shown in Figure 6.

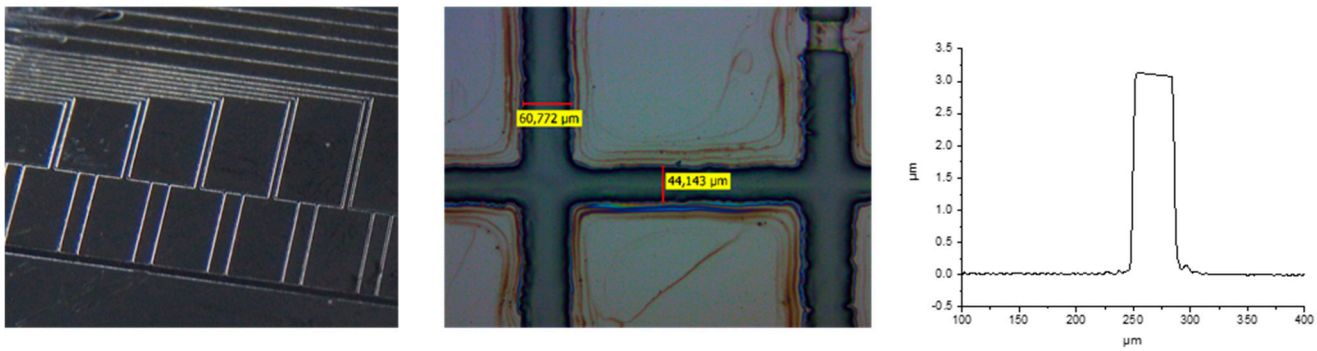

Figure 6. Images of different photolithographic structures prepared via core polymer and surface profiling obtained using Dektak 8 profilometer.

2.3. Composite Waveguiding Materials Containing SiO_2 and MgF_2 Nanoparticles

Inorganic materials possess lower coefficients of thermal expansion and consequently lower TOCs compared to organic materials (polymers). Additionally, some inorganic materials (e.g., MgF_2, AlF_3, SiO_2 and CaF_2) exhibit low or extremely low refractive indices. The combination of inorganic materials in the shape of nanoparticles and organic polymers (nanocomposites) allows tuning of the refractive indices of the resulting waveguide materials. A possible combination of organic and inorganic materials would be a composite in which the inorganic material serves as a filler in a polymeric matrix. Sufficiently small NPs, smaller than 1/20 of the application wavelength (for 1550 nm, smaller than ca. 75–80 nm), produce very weak scattering, and thus this scattering does not make a significant contribution to the optical propagation losses. Therefore, it would be possible, using inorganic NPs, to tune (reduce) the refractive index and TOC. An application of MgF_2 NPs possessing an extremely low refractive index of 1.37 at 1550 nm was rather interesting. The MgF_2 NPs had already been introduced by us into polymeric matrices [29,30]. We demonstrated a decrease in the refractive indices of the resulting nanocomposites [29]. The combination of inorganic and organic materials (nanocomposites) for application in polymer optical waveguides has received little attention so far.

The influence of NPs on the refractive index and TOC is quite understandable theoretically [31], as it is based on their lower n and TOC values compared to organic polymer materials. However, the effect of the same inorganic NPs dispersed in a polymer matrix on optical propagation losses has not been widely studied so far. Inorganic materials constituting the core of NPs usually do not adsorb at telecommunication wavelengths. Therefore, they should exert a positive influence on optical propagation losses. However, an organic shell, usually required to render inorganic NPs dispersible in a polymer matrix, may have a negative or positive influence on the absorption depending on the ligand used for the modification. In addition, if NPs are not sufficiently small or agglomerate in the matrix during their dispersion or following polymer curing, additional scattering will also increase the optical propagation losses.

The introduction of NPs (MgF_2 and SiO_2) was attempted for both types of waveguide polymer materials [1–3]. The general idea for both waveguide material systems is shown in Scheme 8.

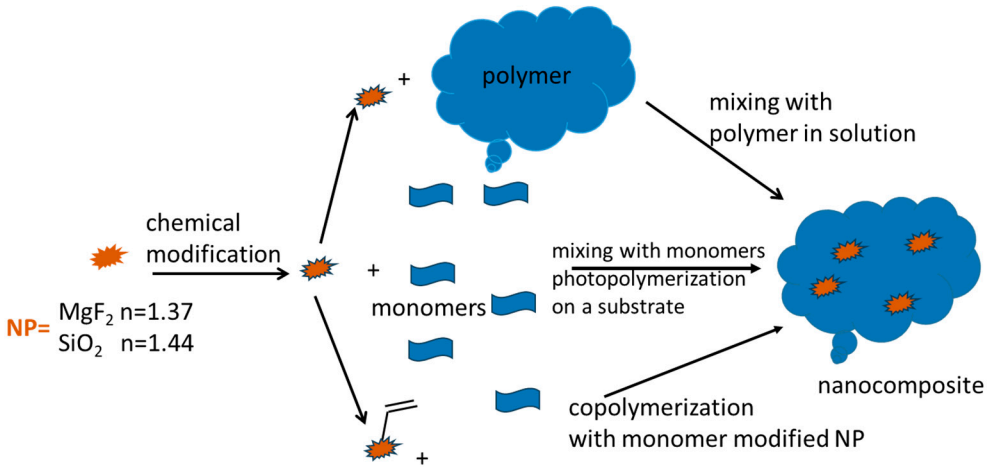

Scheme 8. Schematic representation of nanocomposite fabrication process. It usually starts with NP modification. The top route exhibits the direct blending of NPs into the polymer matrix in solution; the middle route is the direct blending of NPs into the monomer mixture, followed by photochemical radical co-polymerization on the substrate; and the bottom route is the co-polymerization of double-bond-modified NPs together with additional acrylate/vinyl monomers.

SiO_2 NPs were purchased from Nissan Chemical Industries Ltd. (Tokyo, Japan), Evonik Resource Efficiency GmbH and BYK-Chemie GmbH [1,2], while MgF_2 NPs were synthesized in-house.

For the direct introduction of SiO_2 NPs into the monomer mixtures described in Section 2.1 (Scheme 8, bottom route), we used commercially available SiO_2 NP dispersions (Nissan, Evonik and BYK; diameter: ca. 20 nm). The NP dispersions from Nissan and the Nanopol dispersions from Evonik are based on solvents with different boiling points. The solvents in MEK-ST and Nanopol C784 have lower boiling points and therefore are easier to remove by evaporation or distillation if required. Other commercially available materials (Nanocryl and Nanobyk) contain non-fluorinated acrylate monomers as dispersive media. Therefore, their application can increase the optical propagation losses due to a high concentration of C–H bonds.

The experiments with NPs dispersed in solvents (MEK-ST from Nissan and Nanopol C764 and C784 from Evonik) were carried out [2]. Both core (n = 1.48, 1.50) and cladding (n = 1.45) mixtures were formulated successfully by varying the concentration of SiO_2 NPs from 10 to 40 wt%. We also varied the monomer composition to achieve the required refractive index. Most of these mixtures produced layers on the substrates of sufficient optical quality and thickness to obtain a complete optical characterization. The UV-cured polymeric materials exhibited a relatively low TOC of $-(0.6–1.0) \times 10^{-4}$ K^{-1} depending on the composition. Compared to the original acrylate mixture (TOC = $-(1.3–1.5) \times 10^{-4}$ K^{-1}) and the commercial materials form ChemOptics ($-(1.5–2.2) \times 10^{-4}$ K^{-1}) [28], these values were significantly lower. Exemplary measurements of some materials with low TOCs developed by us are shown in Figure 7.

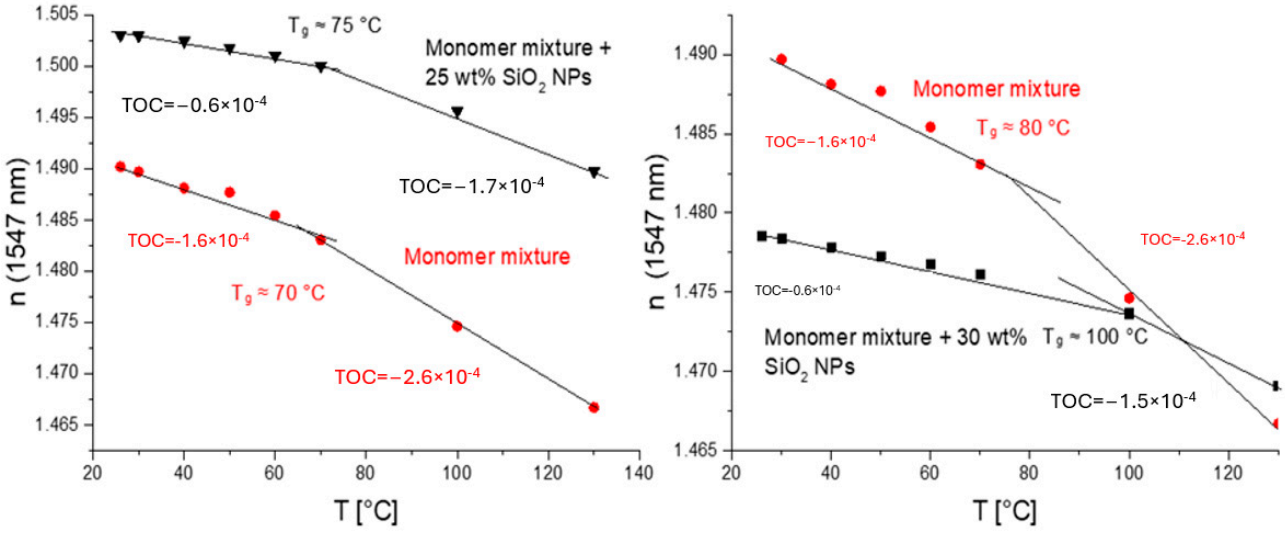

Figure 7. Temperature dependence of n (numbers on the plots are TOCs determined as slopes of linear dependencies): **left**—core acrylate mixture containing 30 wt% of SiO_2 NPs (from Nanopol C784, n = 1.48) and base core acrylate mixture (with $n \approx 1.49$) used to prepare nanocomposite mixture in red; **right**—core acrylate mixture containing 25 wt% of SiO_2 NPs (from Nissan MEK-ST, n = 1.5) and base core acrylate mixture (with $n \approx 1.49$) used to prepare nanocomposite mixture in red.

Thus, the effect of TOC reduction caused by the introduction of an inorganic material, SiO_2 (Nanopol dispersions), is also clearly demonstrated. Also, the glass transition temperature, T_g, is clearly manifested as a kick in the n–T plot. The NPs increased the glass transition temperature by only 20 C in this case (Figure 7, right).

The best samples were comparable with the commercial material from ChemOptics (0.35 dB·cm^{-1} [25]) or Ormocer-type materials from Microresist (0.5–0.7 dB·cm^{-1} at 1547 nm [24,28]). The values of optical propagation losses varied from 0.2 to 1.0 dB·cm^{-1} at 1547 nm. The examples of the optical propagation loss measurements for the nanocomposites are shown in Figure 8. In the case of SiO_2 NP dispersions in organic solvents, we were able to prepare both core and cladding nanomaterials.

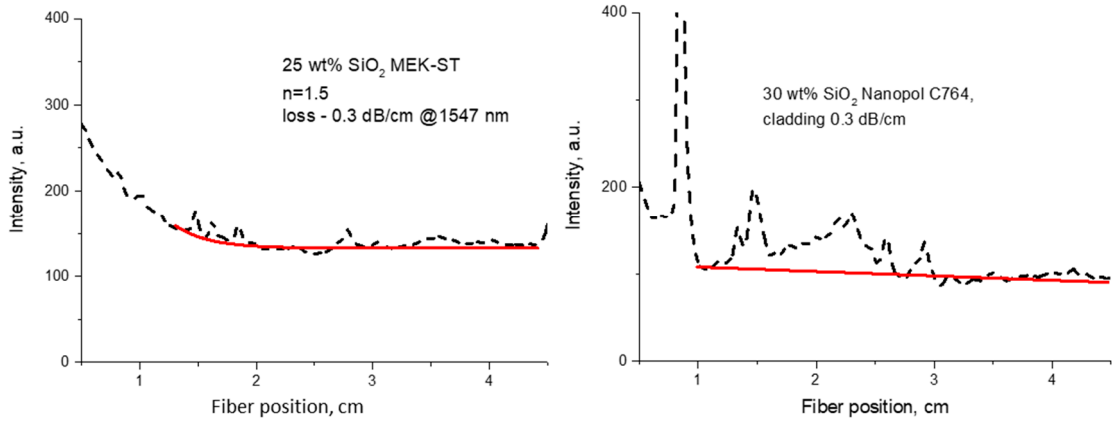

Figure 8. Representations of optical propagation loss measurements for polymer nanocomposites with SiO_2 NPs from different sources: **left**—solvent dispersion for core material (n = 1.5) containing 25 wt% SiO_2 (MEK-ST from Nissan); **right**—cladding material containing 30 wt% SiO_2 (Nanopol C764 from Evonik) (red lines represent exponential fits).

The results based on SiO_2 NP dispersions in acrylate monomers (Nanocryls and Nanobyk) were less conclusive [2]. We also investigated SiO_2 NP monomer formulations with NP concentrations of 20–30 wt%. In this case, a simultaneous increase in the inorganic content and the concentration of C-H bonds in the formulation (addition of non-fluorinated acrylate from the dispersion medium of NPs) should happen. The TOC values were $-(0.8–1.5) \times 10^{-4}$ K^{-1}, thus exhibiting a no clear difference from the materials without NPs. However, despite the additional contribution from non-fluorinated acrylates to optical propagation losses (due to an increase in the concentration of C-H bonds), the best samples exhibited low optical propagation losses of 0.3–0.4 $dB \cdot cm^{-1}$ at 1547 nm.

The fact that such polymers could be used in optical applications under harsh environmental conditions is particularly important for optical glass fibers but also has an implication for optical microchips on the polymer platform. An application in polymer-clad fibers will be considered in Section 3, below. Optical cladding is prepared from a UV cross-linked polymer. This special polymer has high resistance to high optical power and high thermal stability. The material has such requirements because these glass fibers are used, for example, for transmission of laser radiation in surgical lasers and material processing technology, where the transmitted laser power could be up to 100 W. In addition, the fibers for medical lasers can be autoclaved several times with hot steam for healthcare applications [9]. The C–F bonds show high thermal and environmental stability. Therefore, fluorinated polymers (a well-known example being PTFE) typically exhibit increased thermal and media stability compared to their non-fluorinated counterparts [32]. Inorganic materials in the form of NPs could introduce additional stability to the nanocomposites. Therefore, we investigated the influence of harsh environmental conditions (high humidity and high temperature) on the optical propagation losses. The comparison of the original acrylate formulations and the nanocomposites prepared using these formulations for stability in conditions of elevated temperature and/or humidity is shown in Figure 9. The nanocomposites showed better performance at a high temperature (125 °C; Figure 9, right), while under high-humidity and high-temperature conditions (Figure 9, left) the behavior was not good. We can attribute this fact to the probable absorption of water vapor by silica NPs and a consequent decrease in the concentration of C–F bonds.

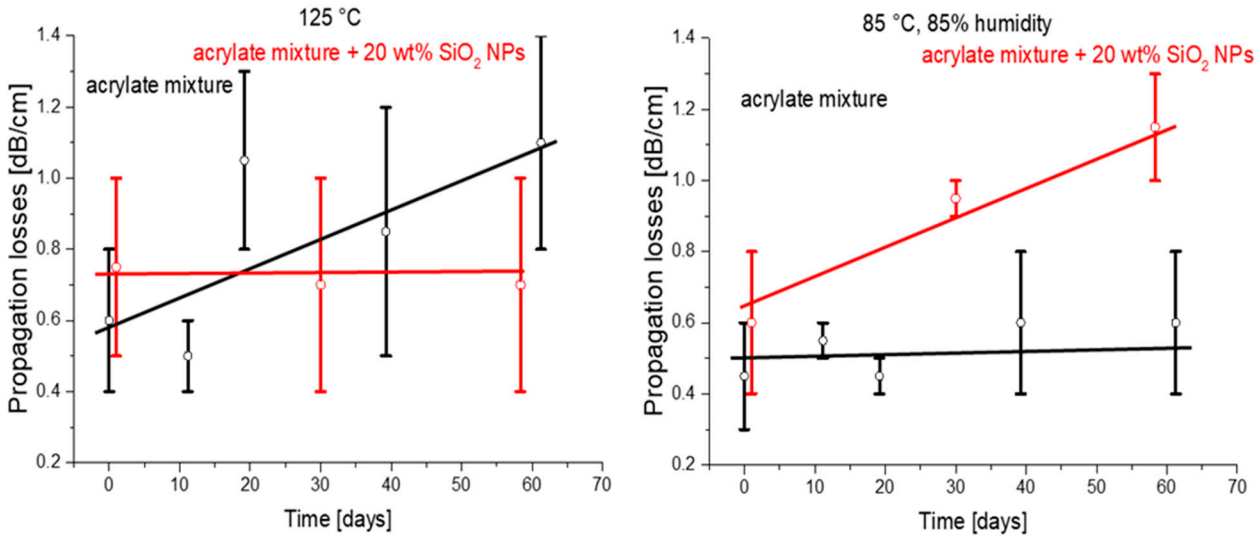

Figure 9. Optical loss investigation of the samples of base material and nanocomposites as a function of climatic conditions (temperature and humidity) (black and red lines represent trends).

MgF_2 nanoparticles were prepared from $Mg(OEt)_2$ by reaction with HF in dry methanol [3]. The NPs were modified with trifluoroacetic acid to render them compatible with optical polymers. Stabilized in this way, MgF_2 NPs were also introduced into monomeric mixtures. Again, the introduction of inorganic NPs led to a decrease in TOC, as shown in Figure 10, left.

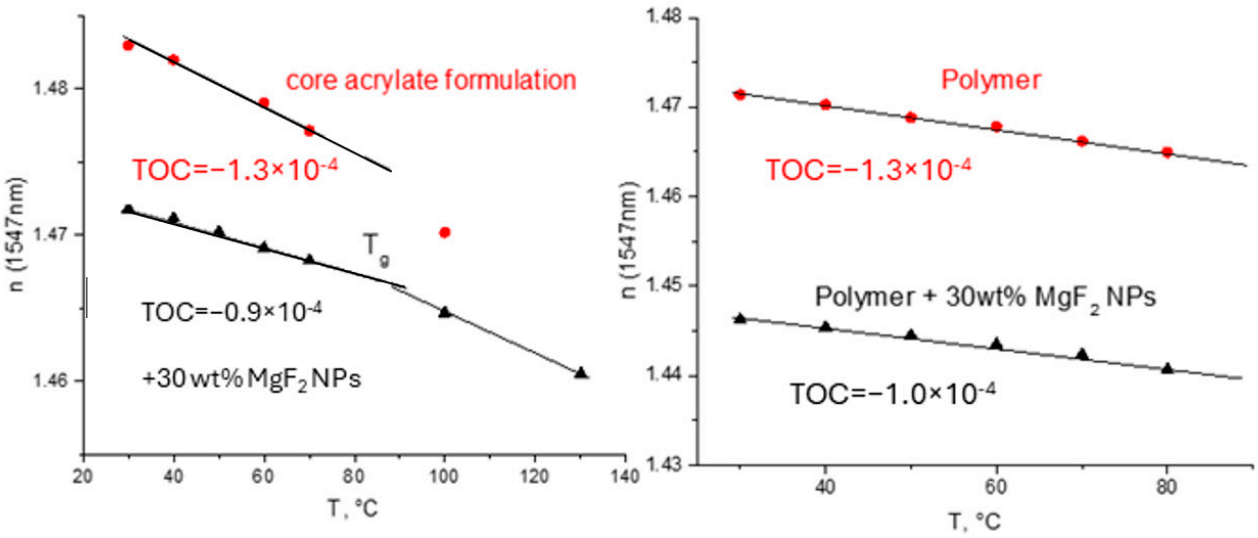

Figure 10. Temperature dependencies of refractive index of acrylate formulation and nanocomposite films (**left**) and polymer and polymer-and-nanocomposite films and (**right**) measured by m-line spectroscopy.

It is also clear that the low-refractive index MgF_2 NPs decreased the refractive index of the resulting polymer films (Figure 10). However, despite visual transparency, the optical propagation loss increased significantly (Figure 11) for the two different acrylate formulations. The light scattering by NPs as a reason for the increase in optical propagation losses is hardly plausible (the NP diameter was ca. 12 nm [33]). Therefore, the absorption of the organic shell consisting of trifluoroacetic acid at 1547 nm could have been responsible for the increase in optical propagation losses.

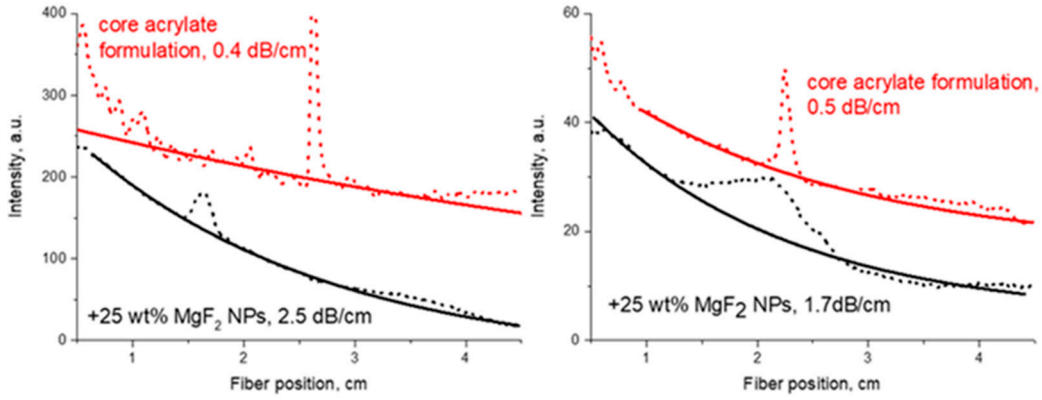

Figure 11. Comparison of optical propagation losses at 1547 nm between polymer material and polymer composites with MgF_2 NPs (solid lines are exponential fits).

Next, we considered nanocomposite materials based on the oxirane-containing polymers described in Section 2.2 [1,3]. Also, low- and extremely low-refractive index MgF_2 and SiO_2 NPs were used (see Scheme 8). In the case of SiO_2 NPs, we attempted to introduce them into the polymer matrix using three different methods, namely, direct blending of the NP dispersion with a polymer solution (similar to monomer mixtures; Scheme 8, upper route), co-polymerization of monomer-modified SiO_2 NPs with other co-monomers (Scheme 8, lower route) and in situ sol–gel formation of similar SiO_2 structures during UV curing and annealing. The formation of similar SiO_2 structures was catalyzed by a photoacid generator using a co-polymer with siloxane groups [34]. The in situ sol–gel formation of similar SiO_2 structures and polymers prepared with monomer-modified NPs is illustrated in Scheme 9.

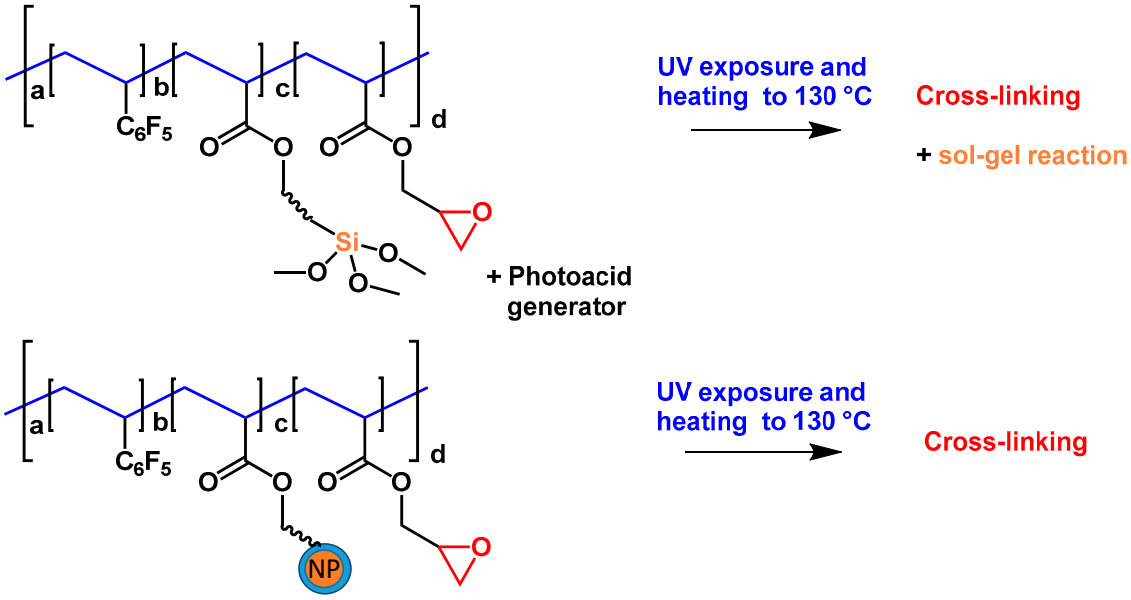

Scheme 9. Schematic representation of co-polymers capable of in situ formation of SiO_2 NPs by sol–gel reaction (**upper route**) and co-polymer containing an NP in a side chain (**lower route**).

SiO_2-containing nanomaterials (sourced from Nissan, Evonik, Nyacol and IOLITEC) were used for direct mixing with oxirane-containing polymers. The MEK-ST and PMA-ST dispersions from Nissan and the porous SiO_2 NPs from IOLITEC (all ca. 20 nm in diameter) were introduced in these polymers. Before processing, the porous NPs were modified with fluorinated silane to render them dispersible. Temperature-dependent spectroscopic ellipsometry was also used in this case to measure the TOC, as it allows measurement of thinner layers (below 1 µm; Figure 12, right) in comparison to m-line spectroscopy (usually thicker than 2–3 µm). Note that TOC should be independent of wavelength. This allowed us to estimate the effect of NP introduction for a broad variety of NPs. A definitive effect of lowering the TOC by the introduction of SiO_2 NPs was registered using the MEK-ST NP dispersion (Nissan; Figure 12).

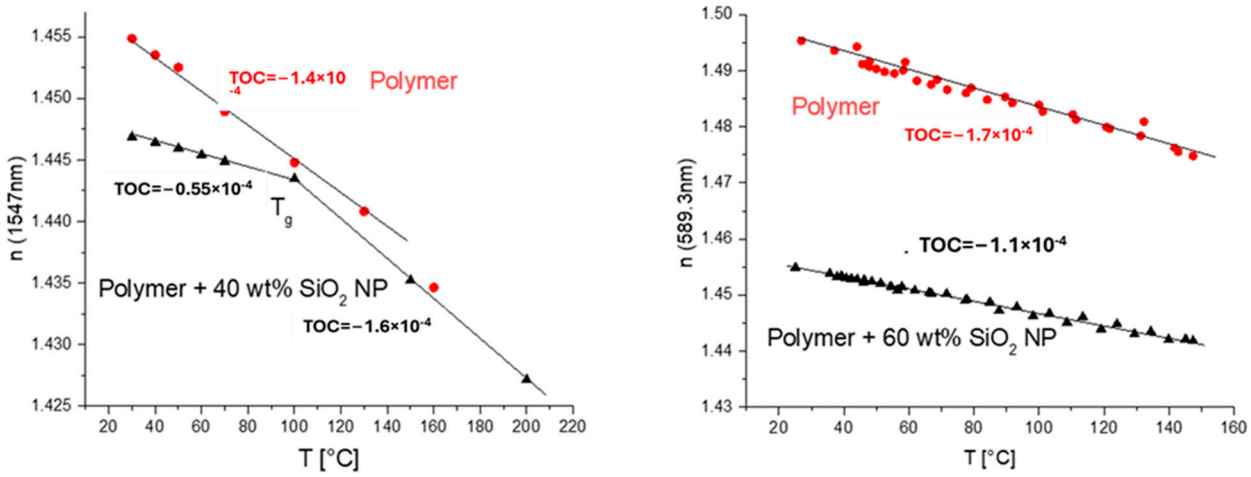

Figure 12. Temperature dependence of refractive index for direct blending of MEK-ST SiO_2 NPs into polymer matrix (red circles—unfilled polymers; black triangles—nanocomposites) for two different oxirane-containing polymers: **left**—m-line spectroscopy; **right**—ellipsometry.

As the next approach, we incorporated NPs into the polymer side chain. For this synthesis, monomer-modified SiO_2 NPs were used as co-monomers in the polymerization. Methacrylate and double-bond-modified NPs, porous NPs modified by 3-(trimethoxysilyl)propyl methacrylate (both from IOLITEC; ca. 20 nm diameter), and S125 (70 nm diameter) and DP5820 NPs (Nyacol; 20 nm diameter) were used in the co-polymerization. Glycidyl methacrylate and trifluoroethyl methacrylate (alternatively, pentafluorostyrene) were used as co-monomers. The presence of NPs in the polymer matrix was proved by TGA (20–30 wt% of SiO_2 residue was determined). TOCs were measured by m-line spectroscopy and ellipsometry, but there was no clear difference. The values for TOC were similar to the values for the basic fluorinated polymers, and a direct comparison was not possible (Figure 13). However, the suppression of the glass transition in the measured temperature range was detected. Similar polymers without NPs have a T_g of ca. 100–120 °C (Figure 13). This could be due to the influence of NPs.

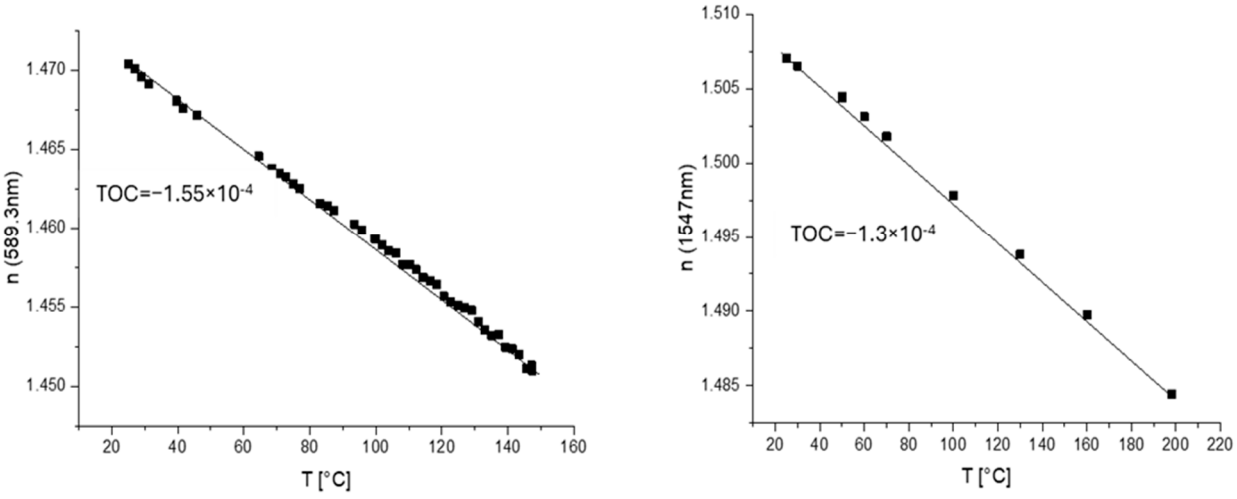

Figure 13. Temperature dependence of refractive index (TOCs of corresponding materials are shown as numbers on the plots) for a polymer incorporating SiO_2 NPs in the side chain. Double-

bond-modified SiO_2 NPs from IOLITEC were used for the synthesis: **left**—m-line spectroscopy; **right**—ellipsometry.

A co-monomer containing a siloxane residue in a side chain was used to prepare SiO_2 NPs inside polymers in situ (Scheme 9, upper route). This monomer was co-polymerized with trifluoroethyl methacrylate or pentafluorostyrene and glycidyl methacrylate. UV curing of the polymer in the presence of a photoacid generator followed by heating to 130 °C leads to the opening of the oxirane rings, as exhibited in the general reaction. Also, the photoacid catalyzes the sol–gel reaction of siloxane groups in the presence of water vapors from the air. This finally leads to the formation of silica-like structures during heating via the evaporation of sol–gel reaction products, namely, ethanol and water. The disadvantage of this route is that the co-polymer cannot be separated and must be used directly from the reaction mixture. In addition, this solution shows only a short shelf time of ca. 1 month, with gelation occurring afterwards due to further sol–gel reaction. M-line measurement exhibited a TOC value of $-(0.95–1.15) \times 10^{-4}$ K^{-1}, and ellipsometry exhibited a TOC value of ca. -1.25×10^{-4} K^{-1} (a steep fall in the refractive index at the beginning was attributed to the loss of residual water) (Figure 14).

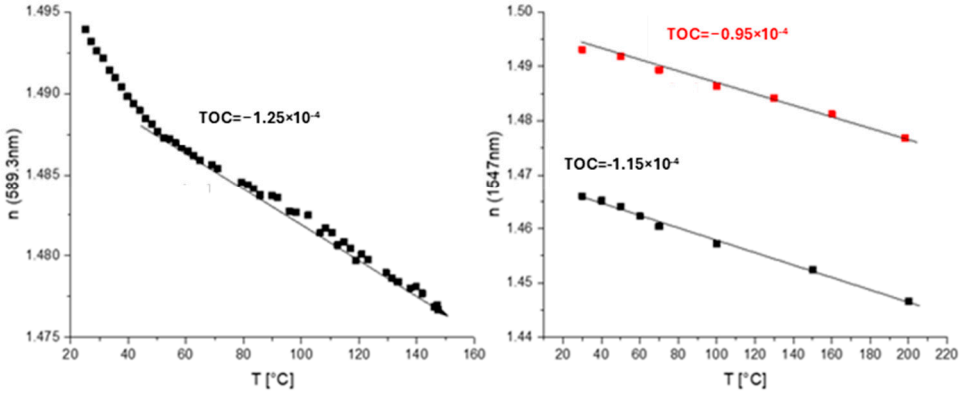

Figure 14. Temperature dependence of n (TOCs of corresponding materials are shown as numbers on the plots) for a polymer with SiO_2 NPs in a side chain obtained by in situ sol–gel reaction: **left**—m-line spectroscopy; **right**—ellipsometry.

In this case, the polymer can be prepared only with silica NPs inside, and there is no basis polymer for comparison. The impact of NPs in situ on the TOC is not clear. However, we did not observe the glass transition of the polymer up to 200 °C. An additional cross-linking via Si–O–Si linkages in situ could be a plausible explanation for this effect.

Examples of optical propagation loss measurements are shown in Figure 15 in comparison to the starting polymer.

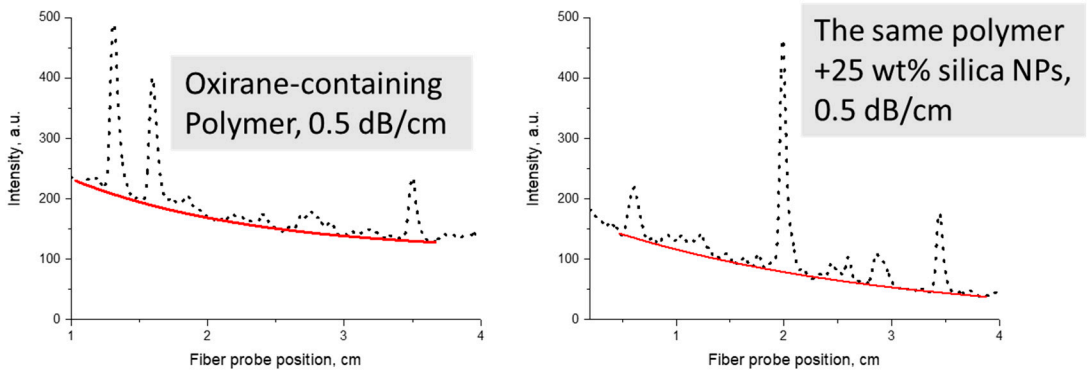

Figure 15. Examples of optical propagation loss measurements at 1547 nm for an oxirane-containing polymer and its nanocomposite with SiO_2 NPs (red lines are exponential fits): **left**—unfilled polymer, **right**—nanocomposite.

Generally, the optical propagation losses in nanocomposite waveguides are comparable with those of the unmodified polymers (Figure 16).

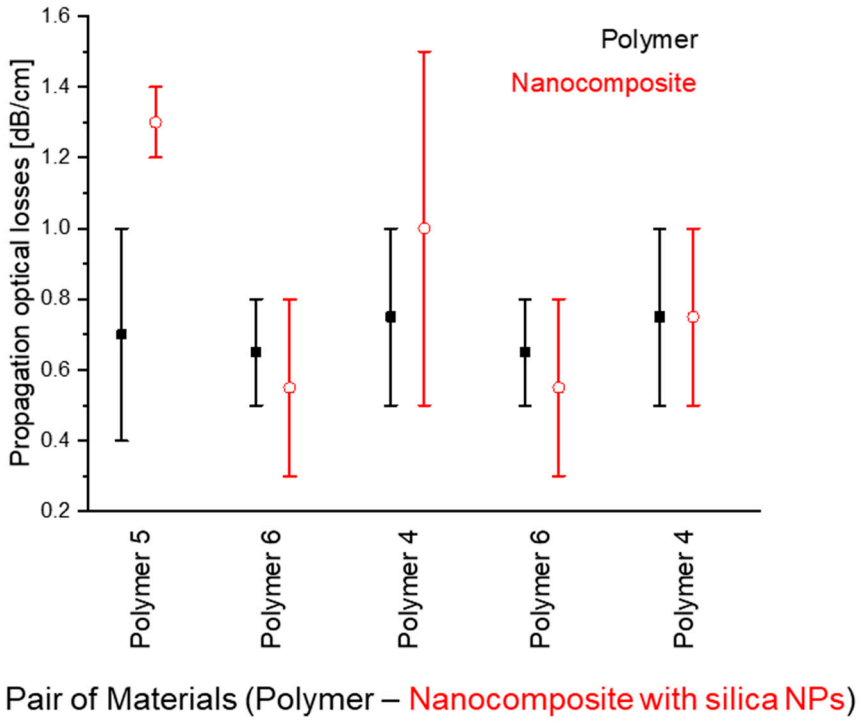

Figure 16. Comparison of the several examples of optical propagation losses between original polymers and polymer composites with SiO_2 NPs (each example corresponds to a pair of materials, one of which is an original polymer (black, full squares) while the other is a nanocomposite based on the same original polymer (red, empty circles)). Value deviations correspond to measurements using either different samples of the same material and/or measurements along different optical passes on the same sample.

The trifluoroacetic acid-modified MgF_2 NPs described above were also introduced into the polymer solution. This resulted in the formation of relatively good-quality films with a thickness of a few micrometers. Unfortunately, some visible scattering appeared after UV curing of the nanocomposite films (apparently, agglomeration of NPs due to

polymer network building). It was still possible to measure the refractive index and TOC (but not optical propagation losses) using the method of m-line spectroscopy (Figure 10, right). It was demonstrated that the introduction of MgF_2 NPs decreases the refractive index and the TOC.

The optical parameter results for the studied polymer and polymer composite materials are collated in Table 1.

Table 1. Optical parameters of polymer materials developed for core and cladding of optical waveguides.

Polymer Material	Propagation Loss at 1547 nm, dB·cm^{-1}	TOC, ×10^{-4} K^{-1}
Monomer materials based on acrylates, core (n = 1.48 and 1.5)	0.3–0.6	−(1.3–1.5)
Monomer materials based on acrylates, cladding (n = 1.45)	0.4–0.5	−(1.3–1.5)
Glycidyl-containing polymer, core (n = 1.48 and 1.5)	0.5–0.7	−(0.65–0.85)
Glycidyl-containing polymer, cladding (n = 1.45)	0.6–0.8	−(0.8–1.0)
Monomer mixtures + SiO_2 NP dispersions in solvents	0.2–1.0	−(0.6–1.0)
Monomer mixtures + SiO_2 NP dispersions in acrylates	0.3–0.4	−(0.8–1.5)
Monomer mixtures + MgF_2 NPs	1.7–2.5	−0.9
Glycidyl-containing polymer + MgF_2 NPs	-	−1.0
Glycidyl-containing polymer + SiO_2 NP dispersions in solvents	0.5–1.0	−(0.55–1.25)
Glycidyl-containing polymer containing SiO_2 NPs in chain	-	−(1.1–1.3)
Glycidyl-containing polymer containing SiO_2 NPs formed in situ	-	−(0.95–1.15)
Reference material, ChemOptics [25]	0.35	−(1.5–2.2)

As a conclusion to this section, we can state that it was possible to fabricate fluorinated polymer waveguiding materials using either double-bond-containing monomer mixtures followed by radical co-polymerization/cross-linking on the substrate or by radical co-polymerization with epoxy monomers followed by crosslinking of polymer films on the substrate initiated by a photoacid generator. Both these materials show relatively low values of optical propagation losses, which is important for their application in passive waveguides for optical microchips on the polymer platform. By the introduction of low-refractive index inorganic nanoparticles of SiO_2 and MgF_2, we were able to reduce the refractive index and TOC for the polymer layer. The first one allowed tuning of the refractive index, while a low TOC is important for the application as a passive waveguide. In the case of SiO_2 NPs, it was also possible to produce polymer materials without compromising optical losses. It was demonstrated that both core and cladding materials could be fabricated on the nanocomposite basis, allowing production of waveguides using only nanocomposites.

3. Fluorinated Polymers as Cladding for Optical Glass Fibers

The experience in the development of materials for optical waveguides [1–5] also provides useful knowledge for the development of polymer cladding materials for optical glass fibers [4–6]. The materials are also based on fluorinated monomers/oligomers cured with UV light. However, in this case, optical polymers with an extremely low refractive index of only 1.39 at 1547 nm are required. Glass fibers coated with a polymer as optical cladding (polymer-clad fibers) are intended for applications in material processing technology and medical technology [35,36]. Hence, only highly fluorinated monomers or oligomers should be taken into consideration. And these monomers/oligomers should be at least partially multifunctional (containing more than one double bond) to enable crosslinking. So, Scheme 5 is valid in this case as well, only the concentration of fluorine atoms should be higher to yield a refractive index much lower than 1.45 (cladding in polymer

waveguides for optical microchips). The importance of environmental stability for polymer-clad glass fibers is described above in Section 2.3, in the discussion of the influence of harsh environmental conditions on the composite materials.

In addition to the refractive index, the viscosity of the formulation is also a very important parameter, since the coating of glass fibers is a continuous process under the application of UV light, leading to photochemical radical cross-linking. Viscosity determines the thickness of UV-cured cladding and the speed of the continuous process. Therefore, the developed monomer/oligomer formulations required optimization for those two parameters. It is possible to achieve different viscosities by mixing lowly viscous but highly fluorinated polyether urethane acrylates with highly viscous acrylates or methacrylate oligomers. Fluorolink® from Solvay SA, which is a UV-curable perfluoro-polyether (PFPE)-urethane methacrylate resin, is the most widely deployed and researched product. Resins can be readily mixed with conventional acrylate monomers/oligomers. As is to be expected, the resulting refractive index depends on the mixture composition determining the fluorine content and on the concentration of the radical photo-initiator, which is a non-fluorinated compound. Therefore, a modular system was developed. It contains fluorinated monomers (high fluorine content, low viscosity) and fluorinated oligomers (low fluorine content, high viscosity). The addition of other modifiers like multifunctional acrylates or other cross-linkers to enhance cross-linking density would change the processing properties (adhesion to the substrate). Highly fluorinated monoacrylates were added to obtain a very low refractive index. A mixture of a bifunctional perfluoropolyether (PFPE)-urethane methacrylate oligomer (Fluorolink® MD700) and a tetra-functional PFPE-urethane acrylate (Fluorolink® AD1700), both Solvay Specialty Polymers (Scheme 10), was found to be practical. To increase the adhesion between the glass fibers and the cladding, silanes were used as adhesion promotors. For better applicability, these materials were co-polymerized with the fluorinated monomers to reduce migration out of the finally cured cladding. Scheme 10 depicts the chemical structures of components according to the technical data sheets of the manufacturers and our NMR spectra. Furthermore, Scheme 10 also depicts the best radical photo-initiator, Omnirad 2100, selected for effective UV-LED curing and cross-linking agents containing silane groups.

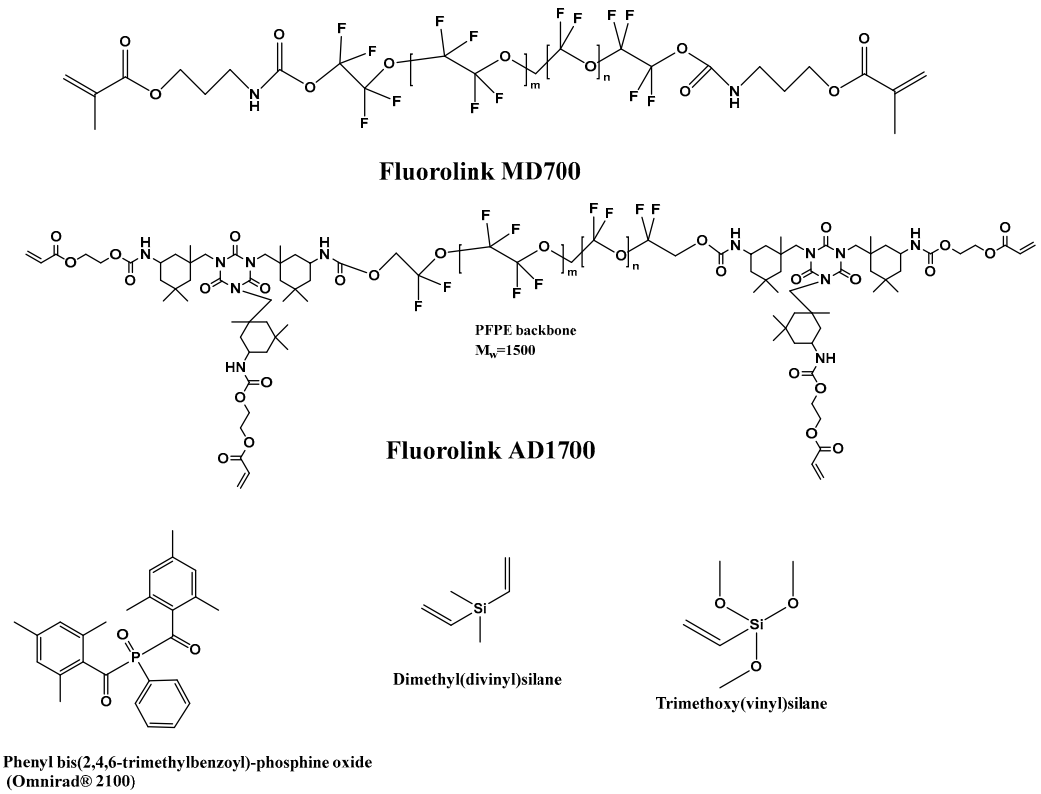

Scheme 10. Representation of molecular structures of fluorinated oligomers, photo-initiator and cross-linking agents for preparation of cladding for glass fibers.

A comparison of the viscosity and the refractive indices of different fluoroacrylate and oligomer formulations is shown in Table 2. The reference was always a commercially available low-refractive index resin system from the glass fiber producer j-fiber GmbH, Jena, Germany, currently used to produce silica-clad glass fibers with curing with a UV lamp. For comparison reasons, the neat Fluorolink AD 1700 and Fluorolink MD 700 were added in Table 2. The reference system is normally cured by mercury lamps at ambient temperature. The application of UV-LEDs instead of mercury vapor lamps containing mercury or noble gases is currently gaining in importance.

Table 2. Viscosity and refractive indices of fluoroacrylates 1 to 3 and references.

No. *	Resin	Viscosity	Refractive Index (20 °C)				
		[mPas, 26 °C]	400.0 nm	486.1 nm	598.3 nm	653.0 nm	704.0 nm
1	Low-index reference from j-fiber	3088.89	1.4074	1.3991	1.3940	1.3920	1.3908
2	Fluorolink AD 1700	22,440.00	1.4428	1.4337	1.4281	1.4259	1.4246
3	Fluorolink MD700	193.80	1.3561	1.3506	1.3471	1.3456	1.3448
4	Fluorolink AD 1700/Fluorolink MD700 = 1/2	990.00	1.3877	1.3805	1.3761	1.3744	1.3733
5	Fluorolink AD 1700/Fluorolink MD700 = 1/1	6677.80	1.4048	1.3980	1.3933	1.3914	1.3903
6	Fluorolink AD 1700/Fluorolink MD700 = 2/3	3216.87	1.3954	1.3885	1.3839	1.3821	1.3810

* Formulations 2 to 6 were prepared utilizing only solvent-free Fluorolink AD1700 and contained 5% Omnirad 2100 photo-initiator.

Formulation No. 6 (Table 2), developed by us, consists of Fluorolink AD 1700 and Fluorolink MD 700, as well as a liquid photo-initiator. The No. 6 formulation and a commercially available low-index coating material (j-fiber GmbH, Jena, Germany) were cured

in a nitrogen atmosphere as films on glass slides. The resulting samples were an object of investigation of the influence of the exposure time (drawing speed) and the type of light source on the degree of conversion, the cross-linking density of the cured polymers and the consequent thermal properties.

Commercial glass-fiber drawing processes, for example, those performed by j-fiber, run at speeds of up to 2000 mmin^{-1}. Therefore, the investigation of conversion and curing behavior is essential for process development. Hence, acrylate formulations with different compositions and developed by employing different radical photo-initiators were cured for different exposure times (different drawing speeds and UV doses) and by using different UV sources (Hg lamp and 390 nm UV-LEDs). The experimental setup is exhibited in Figure 17.

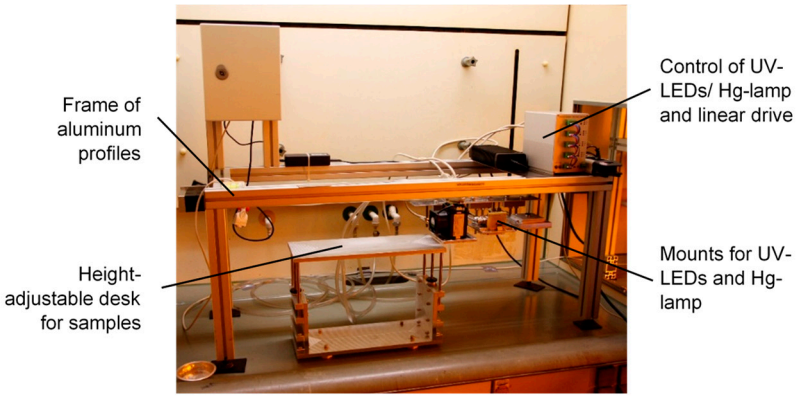

Figure 17. Experimental setup for UV irradiation.

The conversion was determined using FTIR spectroscopy by monitoring the intensity of the 1640 cm^{-1} peak (C=C bond stretching vibrations in the methacrylate group). It was demonstrated that there was almost no difference between the commercial material and the developed formulations at high exposure times over 1 s. With short exposure times, there were significant differences between curing with a Hg lamp and with UV-LEDs. However, the differences between the different formulations and the reference system were only minor (Figure 18).

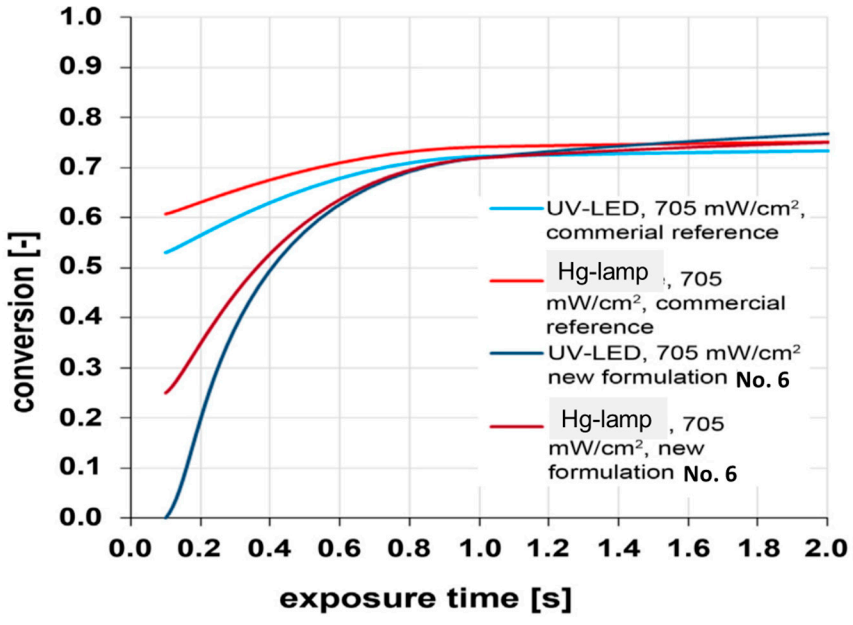

Figure 18. Dependence of UV-curing conversion for commercial mixture and formulation No. 6 on exposure time.

The conversion can reach nearly the value achieved with Hg lamps by increasing the UV intensity of the UV-LEDs. Thus, the highly fluorinated thermosets provide excellent curing behavior (a high degree of conversion) with both UV-LEDs and Hg lamps.

Dynamic Mechanical Analysis (DMA) was also used to investigate the dependence of the conversion of resin formulation No. 6 on the exposure time with UV-LED light. For this mechanical investigation, coatings prepared on glass slides were separated from the substrate to obtain free-standing films. The curves of the storage modulus (*E′*) and the loss factor (*tanδ*) are shown in Figure 19. As expected, an increasing exposure time (UV-LED, 4 Wcm^{-2}, 385 nm) leads to a higher degree of conversion and thus to a higher network density, resulting in a higher modulus of the rubbery plateau. The modulus of the rubbery plateau at the curve is proportional to the cross-linking density [37]. Additionally, the higher network density leads to an increase in the glass transition temperature (T_g) corresponding to the maximum of the loss factor in the curve.

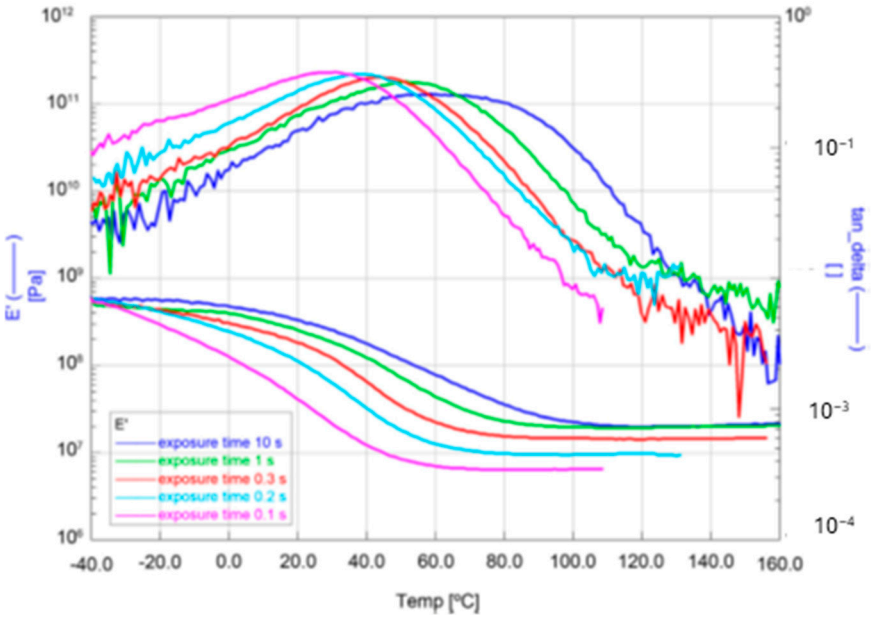

Figure 19. DMA measurements of storage modulus (*E′*) and loss factor (*tanδ*) dependent on temperature for the formulation No. 6 for five different UV-exposure times.

The mechanical properties of the materials were comparable to those of the commercial reference system, but the thermal properties could be improved, and the coating materials can be used at up to 150 °C (Figure 20). Hence, the glass transition temperature of 80 °C of the new material is about 20 °C higher than the glass transition temperature of the reference (60 °C).

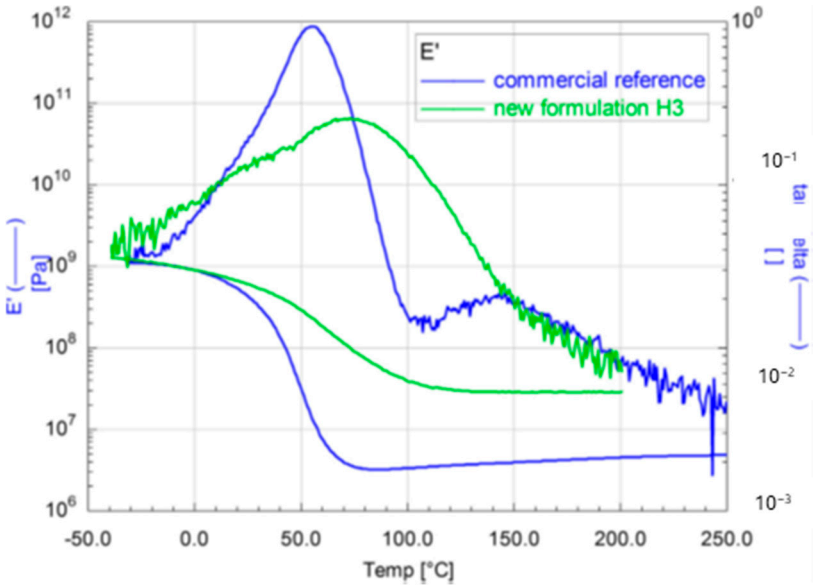

Figure 20. Dynamic Mechanical Analysis of two acrylate-based coating materials: storage modulus (*E′*) and loss factor (*tanδ*) as a function of temperature.

Additionally, the low optical losses of the fibers allow their application in material processing technology and in medical devices (surgery and cosmetics). It has been shown that the developed materials could be autoclaved at least twenty times. Fibers for medical devices using such cladding will in a sense be more sustainable compared to currently commercially available fibers, since they can be re-used more times. Novel cladding materials exhibit excellent thermal properties. In addition, a low water uptake was measured by testing the polymer-clad glass-fibers after multiple cycles in an autoclave. The newly developed coating formulation No. 6 (Table 1) showed no changes after 20 autoclave cycles, whereas currently used materials degraded during the first 5 cycles.

4. Conclusions

The development of new and alternative materials for passive optical waveguides and components and claddings for optical glass fibers is of great interest within the large field of applications of thermosetting UV-curable polymers. It has been shown that for each application a modular system of resins could be compiled to tune the necessary optical, thermal and/or mechanical properties. For optical waveguide materials, it is necessary to develop thermosetting polymers with very low optical propagation losses, specific refractive indices and low thermo-optic coefficients. It has been shown that such materials can be achieved by co-polymerization of different halogenated monomers and glycidyl-functionalized acrylates. The formation of a three-dimensional network structure proceeds via cross-linking reaction of the oxirane groups and irradiation with UV light. This was also possible by the combination of different fluorinated double bonds containing monomers and viscous oligomers, followed by photochemical radical cross-linking on the substrate. In both cases, it was possible to decrease the thermo-optic coefficient using inorganic nanoparticles of SiO_2 and MgF_2 without compromising optical propagation losses. Thus, the determined optical propagation losses of about 0.5 $dB \cdot cm^{-1}$ at 1547 nm were comparable to the value for the reference material, but the thermo-optic coefficient was lower. Also, the development of alternative fluoroacrylates for claddings for optical glass fibers was very successful. The thermosetting polymer containing two commercially available fluorinated oligomers provides an excellent curing behavior, especially for UV-LED curing. It was found that this resin cures very fast and completely by irradiation with 390 nm UV-LEDs. Furthermore, curing printable coatings under air and ambient conditions

with different combinations of 300 nm LEDs and 390 nm LEDs was studied. Despite the availability of many commercial fluorinated materials, future developments are still required to reduce the cost of usually expensive materials and improve their optical and processing properties in the direction of specific applications. In the case of waveguide materials, especially for core materials, a proportion of fluorinated molecules could be changed for other halogenated molecules. This was also shown in our research.

Author Contributions: L.M.G.: methodology, data acquisition, writing—original draft preparation; M.K.: project administration, writing—review and editing; C.D.: funding acquisition, supervision, writing—review and editing. All authors have read and agreed to the published version of the manuscript.

Funding: This research was funded by the German Federal Ministry of Education and Research (Project PolyPhotonics, Support Code 03VKCT1C) and within the consortium Advanced UV for Life (Project InnoUV-Faser, Support Code 03ZZ0124A).

Data Availability Statement: Data are contained within the article.

Conflicts of Interest: The authors declare no conflicts of interest.

References

1. Goldenberg, L.M.; Köhler, M.; Kahle, O.; Dreyer, C. Impact of inorganic nanoparticles on optical properties of low refractive index waveguiding polymers. *Optic. Mater. Expr.* **2020**, *10*, 2987–2997. https://doi.org/10.1364/OME.405700.
2. Goldenberg, L.M.; Köhler, M.; Dreyer, C. SiO_2 Nanoparticles-Acrylate Formulations for Core and Cladding in Planar Optical Waveguides. *Nanomaterials* **2021**, *11*, 1210–1222. https://doi.org/10.3390/nano11051210.
3. Goldenberg, L.M.; Köhler, M.; Dreyer, C.; Krahl, T.; Kemnitz, E. Optical nanocomposites containing low refractive index MgF_2 nanoparticles. *Eur. Phys. J. Appl. Phys*. **2021**, *93*, 404403. https://doi.org/10.1051/epjap/2021200298.
4. Köhler, M.; Goldenberg, L.M.; Pithart, C.; Dreyer, C. UV-Curable Thermosetting Polymers for (Optical) Coatings and Photonics. In Proceedings of the 2017 RadTech Europe Conference & Exhibition 2017, Prague, Czech Republic, 17–19 October 2017.
5. Dreyer, C.; Köhler, M.; Schrader, S.; Yao, H. Chapter 9—Fluorinated thermosetting resins for photonic applications. In *Fascinating Fluoropolymers and Their Applications*; Ameduri, B., Fomin, S., Eds.; Elsevier: Amsterdam, The Netherlands, 2020; pp. 269–335. https://doi.org/10.1016/B978-0-12-821873-0.00009-6.
6. Dreyer, C.; Motoc, D.L.; Köhler, M.; Goldenberg, L. UV LED Curable Perfluoropolyether (PFPE)-Urethane Methacrylate Transparent Coatings for Photonic Applications: Synthesis and Characterization. *Polymers* **2023**, *15*, 2983. https://doi.org/10.3390/polym15142983.
7. Ziemann, O.; Krauser, J.; Zamzow, P.E.; Daum, W. *POF-Handbuch: Optische Kurzstrecken-Übertragungssysteme*; Springer: Berlin/Heidelberg, Germany, 2008; pp. 155–189.
8. Toray: Technical Bulletin—Toray Polymer Optical Fiber Cord, Typ: PF, PG, PHK, available online https://easypdfs.cloud/downloads/4919257-Technical%20Data%20Sheet%20Toray (accessed on 7 February 2025).
9. Leoni Fiber-Optics Katalog. p. 168, available online: https://pdf.directindustry.de/pdf/leoni-ag/lichtwellenleiter-kabel/14158-24334.html (accessed on 7 February 2025).
10. Watanabe, T.; Ooba, N.; Hida, Y.; Hikita, M. Influence of humidity on refractive index of polymers for optical waveguide and its temperature dependence. *Appl. Phys. Lett*. **1998**, *72*, 1533–1535. https://doi.org/10.1063/1.120574.
11. Usui, M.; Hikita, M.; Watanabe, T.; Amano, M.; Sugawara, S.; Hayashida, S.; Imamura, S. Low-loss passive polymer optical waveguides with high environmental stability. *J. Lightwave Technol.* **1996**, *14*, 2338–2343.
12. Mizuno, H.; Sugihara, O.; Kaino, T.; Okamoto, N.; Hosino, M. Low-loss polymeric optical waveguides with large cores fabricated by hot embossing. *Opt. Lett*. **2003**, *28*, 2378–2380.
13. Ma, H.; Yen, A.K.-Y.; Dalton, L.R. Polymer-Based Optical Waveguides: Materials, Processing, and Devices. *Adv. Mater*. **2002**, *14*, 1339–1365. https://doi.org/10.1002/1521-4095(20021002)14:19%3C1339::AID-ADMA1339%3E3.0.CO;2-O.
14. Zhang, Z.; Zhao, P.; Lin, P.; Sun, F. Thermo-optic coefficients of polymers for optical waveguide applications. *Polymer* **2006**, *47*, 4893–4896.
15. Kane, C.F.; Krchnavek, R.R. Benzocyclobutene optical waveguides. *IEEE Photonics Technol. Lett.* **1995**, *7*, 535–537. https://doi.org/10.1109/68.384535.

16. Smith, D.W.; Chen, S.; Kumar, S.M.; Ballato, J.; Topping, C.; Shah, H.V.; Foulger, S.H. Perfluorocyclobutyl copolymers for microphotonics. *Adv. Mater*. **2002**, *14*, 1585–1589. https://doi.org/10.1002/1521-4095(20021104)14:21%3C1585::AID-ADMA1585%3E3.0.CO;2-S.
17. Ballato, J.; Foulger, S.H.; Smith, D.W., Jr. Optical properties of perfluorocyclobutyl polymers. II. Theoretical and experimental attenuation. *JOSA B* **2004**, *21*, 958–967.
18. Jin, J.; Topping, C.M.; Chen, S.; Ballato, J.; Foulger, S.H.; Smith, D.W. Synthesis and comparison of CF3 versus CH3 substituted perfluorocyclobutyl (PFCB) networks for optical applications. *J. Polym. Sci. A* **2004**, *42*, 5292–5300. https://doi.org/10.1002/pola.20342.
19. Aharoni, S. M. Fluoropolymers and fluoropolymer coatings**,** US Patent No. 5183839, 16 September 1991.
20. Dreyer, C.; Schneider, J.; Göcks, K.; Beuster, B.; Bauer, M.; Keil, N.; Yao, H.H.; Zawadzki, C. New Reactive Polymeric Systems for Use as Waveguide Materials in Integrated Optics. *Macromol. Symp*. **2003**, *199*, 307–319. https://doi.org/10.1002/masy.200350926.
21. Dreyer, C.; Frommberger, M. Thermosets for Optical Applications—An Overview with Selected Examples. Thermosets 2009, from Monomers to components. *Micromater. Nanomater.* **2009**, *11*, 46–51.
22. Watanabe, T.; Ooba, N.; Hayashida, S.; Kurihara, T.; Imamura, S. Polymeric optical waveguide circuits formed using silicone resin. *J. Lightwave Technol*. **1998**, *16*, 1049.
23. Toyoda, S.; Ooba, N.; Hikita, M.; Kurihara, T.; Imamura, S. Propagation loss and birefringence properties around 1.55 μm of polymeric optical waveguides fabricated with cross-linked silicone. *Thin Solid Films* **2000**, *370*, 311–314. https://doi.org/10.1016/S0040-6090(00).
24. Buestrich, R.; Kahlenberg, F.; Popall, M.; Dannberg, P.; Müller-Fiedler, R.; Rösch, O. ORMOCER® s for optical interconnection technology. *J. Sol-Gel Sci. Technol.* **2001**, *2*, 181–186. https://doi.org/10.1023/A:1008755607488.
25. Available online: http://www.chemoptics.co.kr/en/sub/technical/data.php?mode=view&inSeq=6& (accessed on 7 February 2025).
26. Zhang, Z.; Mettbach, N.; Zawadzki, C.; Wang, J.; Schmidt, D.; Brinker, W.; Grote, N.; Schell, M.; Keil, N. Polymer-based photonic toolbox: Passive components, hybrid integration and polarisation control. *IET Optoelectron.* **2011**, *5*, 226–232. https://doi.org/10.1049/iet-opt.2010.0054.
27. Zawadzki, C.; Schirmer, M. Der Wellenleiter-Chip—Photonische Bauelemente aus Polymeren. *Photonik* **2018**, *1*, 43.
28. Prajzler, V.; Jasek, P.; Nekvindova, P. Inorganic–organic hybrid polymer optical planar waveguides for micro-opto-electro-mechanical systems (MOEMS). *Microsyst. Technol*. **2019**, *25*, 2249–2258. https://doi.org/10.1007/s00542-018-4105-x.
29. Noack, J.; Fritz, C.; Flügel, C.; Hemmann, F.; Gläsel, H.-J.; Kahle, O.; Dreyer, C.; Bauer, M.; Kemnitz, E. Metal fluoride-based transparent nanocomposites with low refractive indices. *Dalton Trans*. **2013**, *42*, 5706–5710. https://doi.org/10.1039/c3dt32652g.
30. Noack, J.; Schmidt, L.; Gläsel, H.-J.; Bauer, M.; Kemnitz, E. Inorganic–organic nanocomposites based on sol–gel derived magnesium fluoride. *Nanoscale* **2011**, *3*, 4774–4779. https://doi.org/10.1039/c1nr10843c.
31. Zou, H.; Wu, S.; Shen, J. Polymer/Silica Nanocomposites: Preparation, Characterization, Properties, and Applications. *Chem. Rev*. **2008**, *108*, 3893–3957. https://doi.org/10.1021/cr068035q.
32. *Fluoropolymers 1: Synthesis*; Hougham, G.G., Cassidy, P.E., Johns, K., Davidson, T., Eds.; Kluwer Academic Publishers, New York/Boston/Dordrecht/London/Moscow: 2002; p. 330.
33. Noack, J.; Emmerling, F.; Kirmse, H.; Kemnitz, E. Sols of nanosized magnesium fluoride: Formation and stabilisation of nanoparticles. *J. Mater. Chem.* **2011**, *21*, 15015–15021. https://doi.org/10.1039/C1JM11943E.
34. Chemtob, A.; Versace, D.-L.; Belon, C.; Croutxé-Barghorn, C.; Rigolet, S. Concomitant organic− inorganic UV-curing catalyzed by photoacids. *Macromolecules* **2008**, *41*, 7390–7398. https://doi.org/10.1021/ma801017k.
35. Chang, S.; Lee, D.; Oh, J. UV-Curable Resin Composition for Cladding Optical Fiber. U.S. Patent No. US 2006/0067638 A1, 16 May 2006.
36. Bishop, T.; Gan, G. LED Curing of Radiation Curable Optical Fiber Coating Compositions. U.S. Patent No. WO 2011/075549, 23 June 2011.
37. Treloar, L.G.R. *The Physics of Rubber Elasticity*; Oxford University Press: New York, NY, USA, 1975.